Summer School "**Severe Convective Weather: Theory and Applications**"
Lecce, Italy, September 2012

III. Atmospheric Convective Boundary Layer with Wind Shears

Evgeni Fedorovich

University of Oklahoma, School of Meteorology

Outline

- Phenomenology of sheared CBLs
- Historical overview of CBL studies
- Basic questions and unresolved issues
- DNS and LES of sheared CBLs
- Parameterization of convective entrainment
- Answers (to some of) basic questions and solutions (to some of) unresolved problems

Convective boundary layer (CBL) above a heated surface

Dry (or clear) **atmospheric CBL** is a **turbulently mixed boundary layer** with turbulence dominantly generated by heating from below and wind shearbeing the secondary turbulence production mechanism

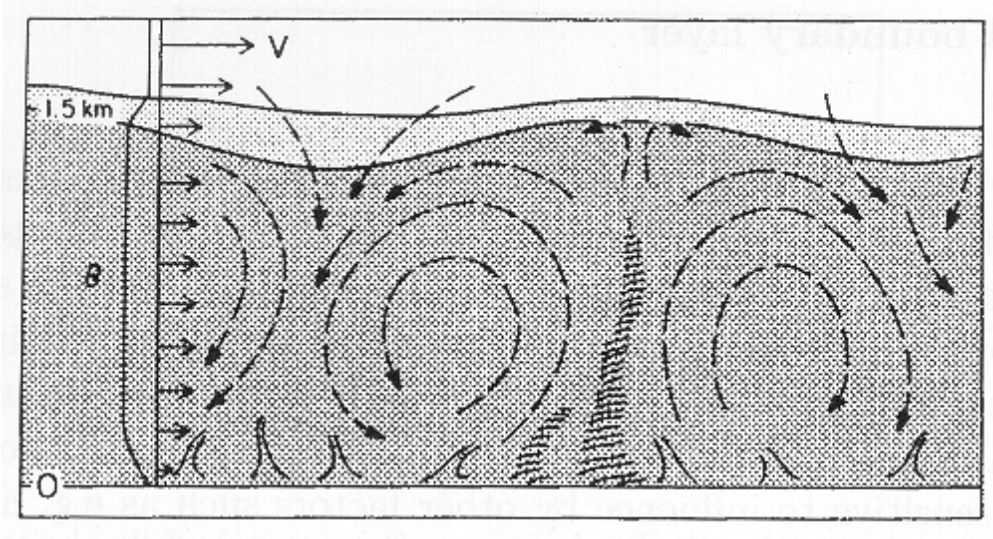

Structure of temperature and wind fields in the atmospheric CBL

(after John Wyngaard)

Potential temperature field in the inversion-capped CBL (DNS visualization)

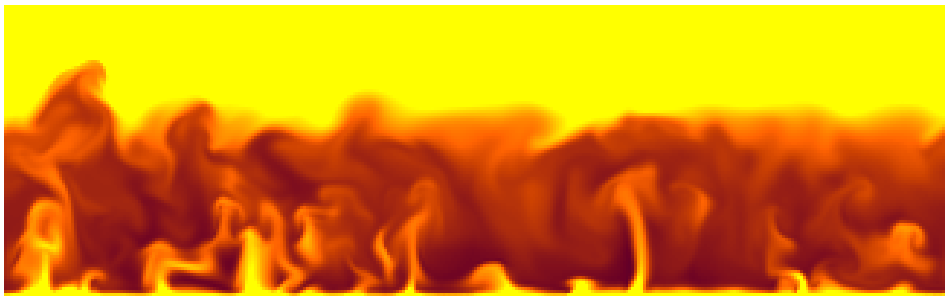

CBL without wind shear

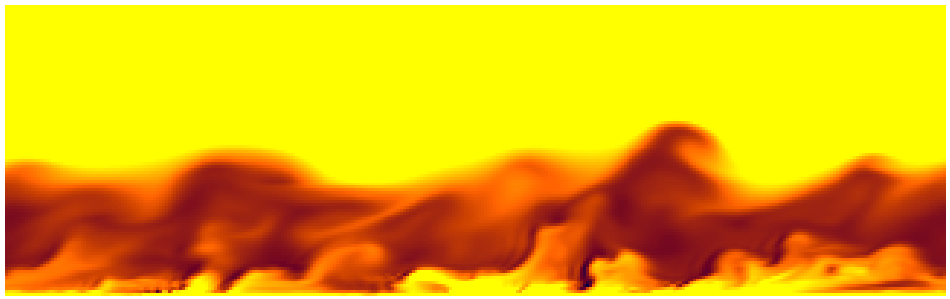

CBL with wind shear

Flow structure in sheared vs. shear-free CBL

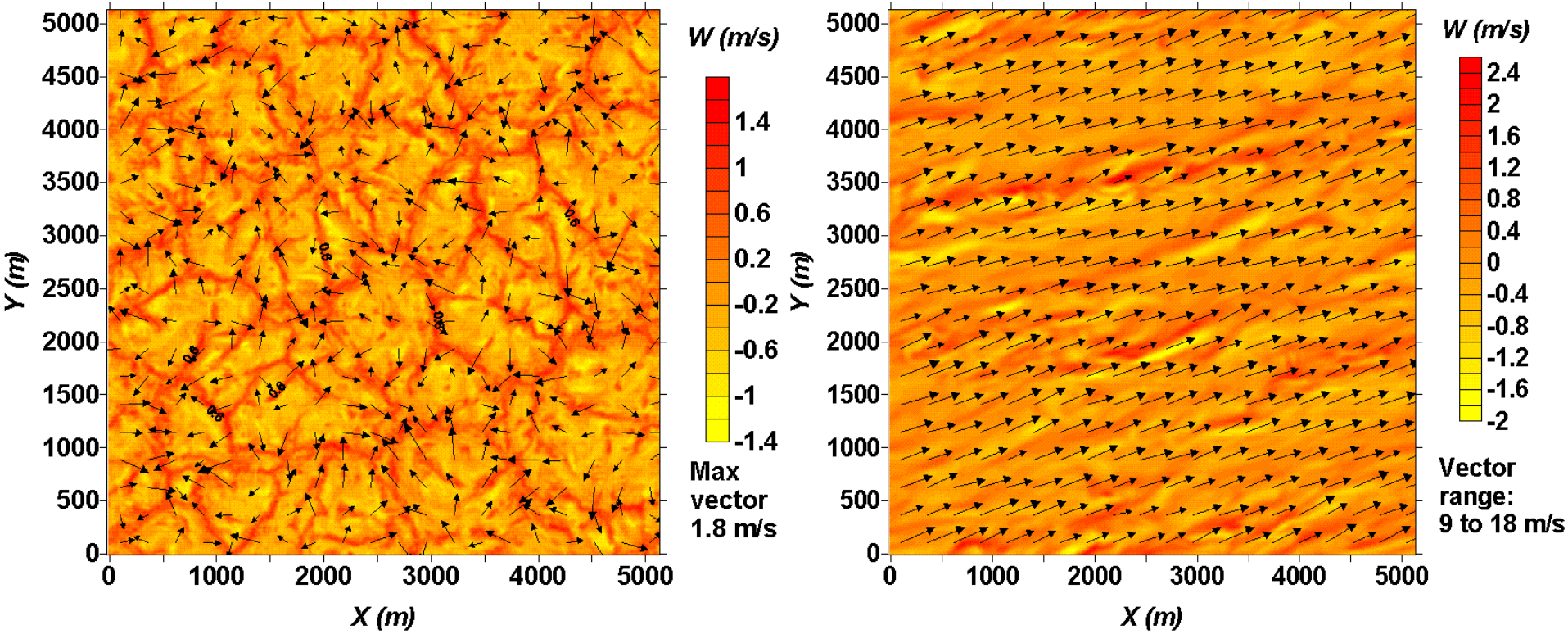

Shear-free CBL **Sheared barotropic CBL**

Vectors: u and v; color scale: w

Note:

- quasi-hexagonal cell-like structures in the shear-free CBL
- horizontal rolls oriented along the mean flow in the sheared CBL

Mean CBL velocity and buoyancy profiles

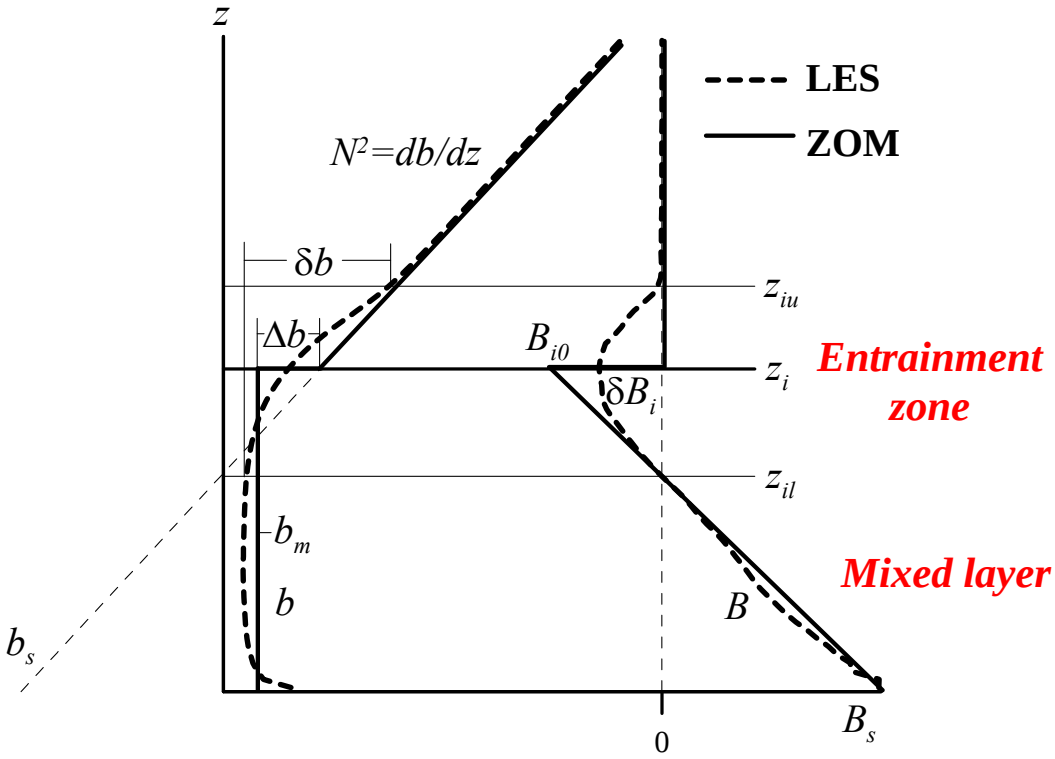

Buoyancy $b = (g/\theta_0)(\theta - \theta_r)$

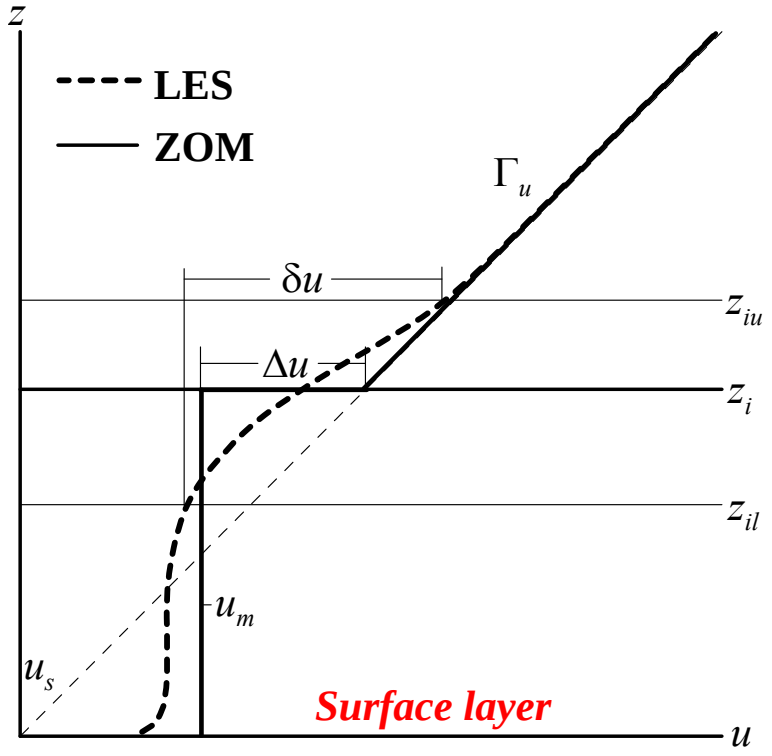

Velocity

CBL may be subdivided vertically into three regions:

Surface layer − ≈10% of the CBL depth.

Mixed layer − main portion of the CBL with all fields well mixed.

Entrainment (or ***interfacial***) ***layer*** − stably stratified region.

Early model/conceptual CBL studies

Shear-free CBL:

Ball (1960) assumed 100% of the TKE available for entrainment.

Lilly (1968) estimated available TKE ranging from zero to 100%.

Betts, Carson, Tennekes, Stull (1973): attempts to determine this fraction.

Generally agreed-upon value for shear-free CBL is **≈0.2**.

Sheared CBL:

Zeman and Tennekes (1977) accounted for the dissipation of shear-generated TKE.

Price et al. (1978) used oceanic data to estimate shear-generated TKE available for entrainment; found the fraction to be **≈0.7**. This number has been used in many later studies.

A popular belief: in a sheared CBL, the entrainment flux ratio should be larger than the shear-free value of 0.2.

CBL observations and measurements

Studies of CBL with soundings (Hoxit 1974; Arya and Wyngaard 1975; Garratt and Wyngaard 1982; Lemone et al. 1999; and Angevine et al. 2001).

Measurements of surface wind shear in CBL (Lemone 1973; Pennel and Lemone 1974).

Higher-order CBL turbulence moments/budgets from aircraft, tether sondes, or radar (Lenschow et al. 1970-1980; Kaimal et al. 1976; Caughey and Palmer 1979; Brost et al. 1982; Flamant et al. 1997).

Atmospheric estimates of CBL entrainment ratios (Grossman 1992; Betts et al. 1992-1996; Davis et al. 1997; Angevine 1999; Margulis and Entekhabi 2004).

CBL depth evolution (Mahrt and Lenschow 1976; Stull 1976; Zeman Tennekes, Driedonks 1977, 1981, 1982; Boers et al. 1984; Batchvarova and Gryning 1991, 1994; and Pino et al. 2003).

Common difficulties with atmospheric data:

1. How to isolate entrainment from other CBL-growth mechanisms?
2. Hard to obtain reliable higher-order turbulence statistics.

Laboratory CBL studies: water tanks

No mean shear: buoyancy-produced turbulence (Turner 1965; Deardorff et al. 1969-1985) or mechanical agitation (Turner 1968).

Surface shear, no buoyancy: Kato and Phillips (1969); Wu (1973); Long (1975); Deardorff and Willis (1982).

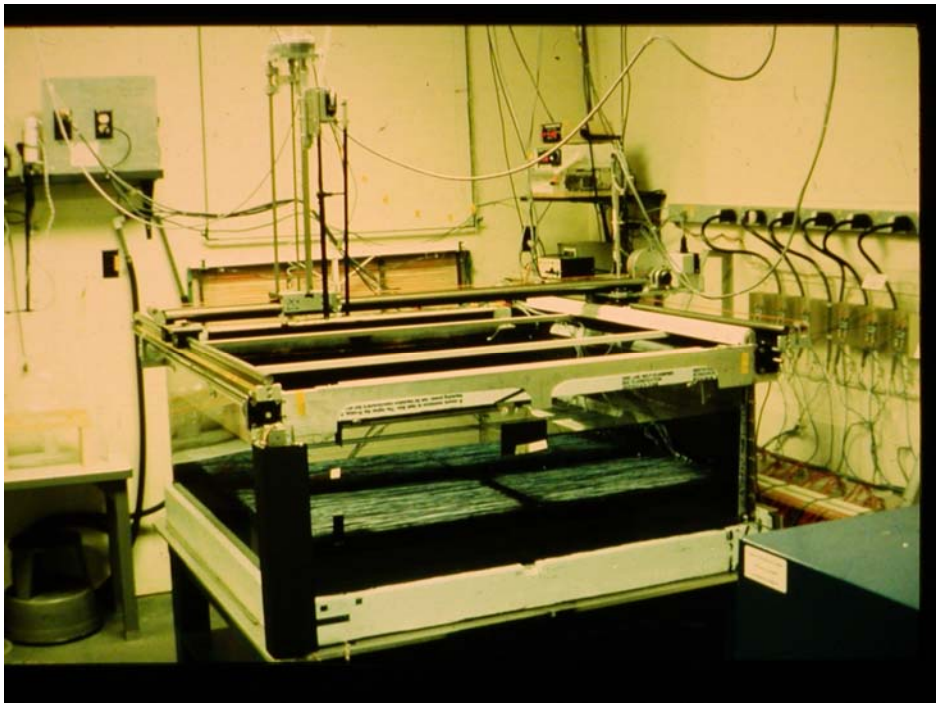

Replica of Deardorff et al. tank

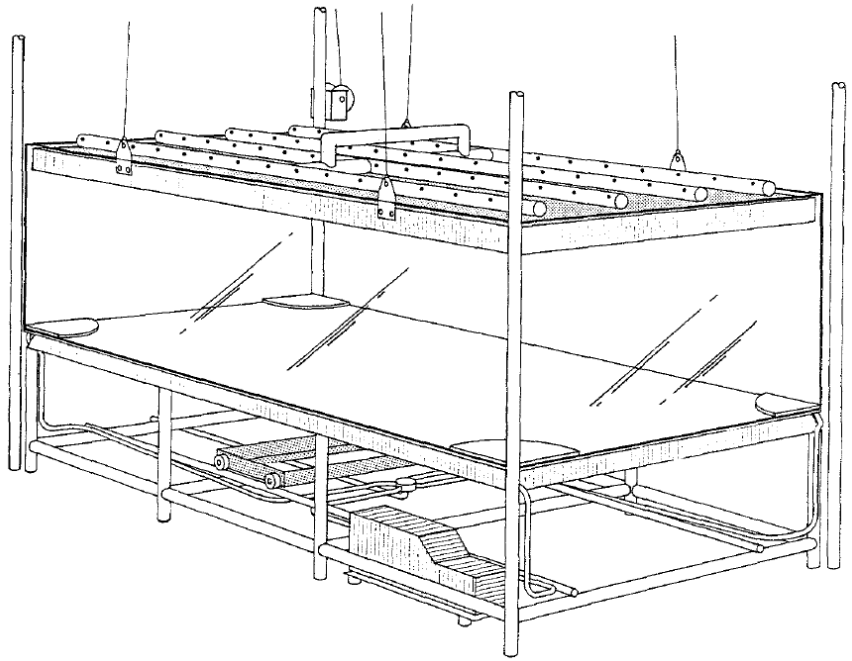

Saline tank of CSIRO (Australia)

None of water-tank studies, however, studied effects of shear and buoyancy forcings occurring in combination.

Wind tunnel models of sheared CBLs

Lots of data from the 1990s and 2000s!

(e.g., **Fedorovich et al.** in Germany and **Ohya et al.** in Japan)

Thermally stratified wind tunnel of UniKA (Germany)

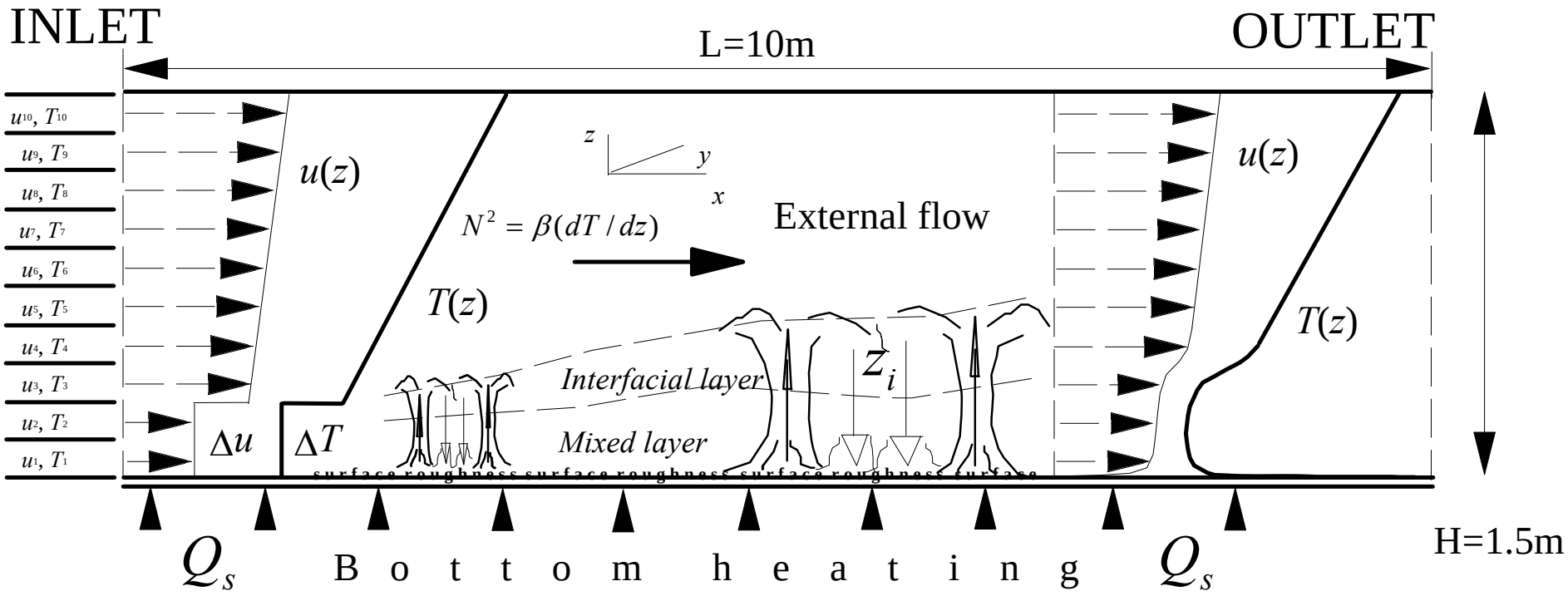

Main problem: **it is flow divergence, not the entrainment,** that primarily drives CBL depth evolution!

Numerical modeling/simulation of CBL

Simulation versus **modeling** of turbulence (Wyngaard 1998)**:**

Simulation resolves all (or most energy-carrying) turbulent motions.

Model deals with integral effect of turbulent motions.

Deardorff (1970) pioneered the use of **large eddy simulation** (**LES**) in the atmospheric CBL studies.

Shear-free CBL: Deardorff (1970-1980); Moeng and Wyngaard (1984); Wyngaard and Brost (1984); Mason (1989); Schmidt and Schumann (1989); Sorbjan (1996); Lewellen and Lewellen (1998); Sullivan et al. (1998); Van Zanten et al. (1999); Fedorovich et al. (2004).

Sheared CBL: studies focusing the CBL structure (Deardorff 1972; Sykes and Henn 1989; Kanna and Brasseur 1998), turbulence dynamics (Moeng and Sullivan 1994), velocity field statistics (Brown 1996), turbulence spectra (Otte and Wyngaard 2001), CBL evolution (Pino et al. 2003), baroclinicity effects (Sorbjan 2004), and instabilities at the CBL top (Kim et al. 2003).

Main problem with numerical simulations:

"It is not a real stuff!" (to which extent should one trust DNS/LES?)

Outstanding questions regarding sheared CBL dynamics

- How does the CBL growth rate depend on shear in relation to the buoyancy forcing?
- What is relative role of entrainment zone shear versus surface shear in the CBL turbulence dynamics?
- What fraction of shear-generated TKE in CBL escapes dissipation and is available for entrainment?
- What is the buoyancy to shear TKE production ratio in the upper portion of sheared CBL, for instance, in terms of Richardson numbers?
- Is there any critical parameter (number) that controls dynamics of entrainment into sheared CBL?
- How well do predictions of entrainment in sheared CBLs by existing bulk models compare with numerical data for characteristic atmospheric ranges of CBL forcings?

CBL governing equations in Boussinesq form

***Equations of motion*:**

$$\frac{\partial v_i}{\partial t} + v_j \frac{\partial v_i}{\partial x_j} = -\frac{\partial \pi}{\partial x_i} + \frac{g}{\theta_c}(\theta - \theta_r) + \varepsilon_{ij3} f (v_j - V_{gj}) + \nu \frac{\partial^2 v_i}{\partial x_j \partial x_j},$$ **where**

$\pi = (p - p_r)/\rho_c$ is **normalized pressure deviation**,

geostrophic wind vector $\mathbf{V}_g = (V_{g1}, V_{g2})$ is defined through

$$-\frac{1}{\rho_c}\frac{\partial p_r}{\partial x_1} + f V_{g2} = 0, \quad -\frac{1}{\rho_c}\frac{\partial p_r}{\partial x_2} - f V_{g1} = 0,$$

θ_r and p_r are **environmental values** of θ and p,

θ_c and ρ_c **are constant reference values of** θ and ρ,

***Heat balance equation*:**

$$\frac{\partial \theta}{\partial t} + v_i \frac{\partial \theta}{\partial x_i} = \nu_h \frac{\partial^2 \theta}{\partial x_i \partial x_i}.$$

Filtered $(\widetilde{\ldots})$ governing equations in LES

$$\frac{\partial \widetilde{v}_i}{\partial t}+\frac{\partial \widetilde{v}_i \widetilde{v}_j}{\partial x_j}=-\frac{\partial \tilde{\pi}}{\partial x_i}+\frac{g}{\theta_c}(\tilde{\theta}-\theta_r)+\varepsilon_{ij3} f(\tilde{v}_j-V_{gj})+\nu\frac{\partial^2 \widetilde{v}_i}{\partial x_j \partial x_j}-\frac{\partial}{\partial x_j}(\widetilde{v_i v_j}-\widetilde{v}_i\widetilde{v}_j),$$

$$\frac{\partial \widetilde{v}_i}{\partial x_i}=0,$$

$$\frac{\partial \tilde{\theta}}{\partial t}+\frac{\partial \tilde{\theta}\widetilde{u}_j}{\partial x_j}=\kappa\frac{\partial^2 \tilde{\theta}}{\partial x_j \partial x_j}-\frac{\partial}{\partial x_j}(\widetilde{\theta u_j}-\tilde{\theta}\widetilde{u}_j),$$

where $\widetilde{u_i u_j}-\widetilde{u}_i\widetilde{u}_j=-\tau_{ij}^s$ subgrid kinematic momentum flux,

$\widetilde{\theta u_j}-\tilde{\theta}\widetilde{u}_j=Q_j^s$ subgrid kinematic heat flux.

In our LES studies of CBL we mostly employ subgrid TKE model of Deardorff (1980), see Lecture II.

Initial flow fields for idealized CBL simulations

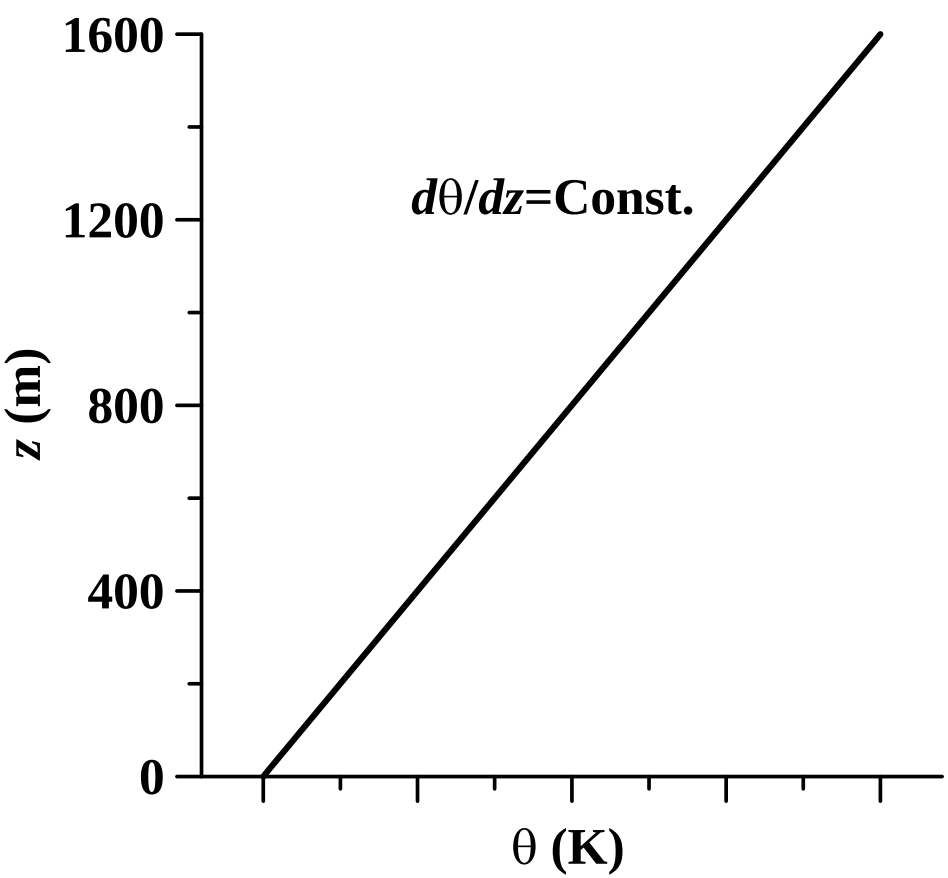

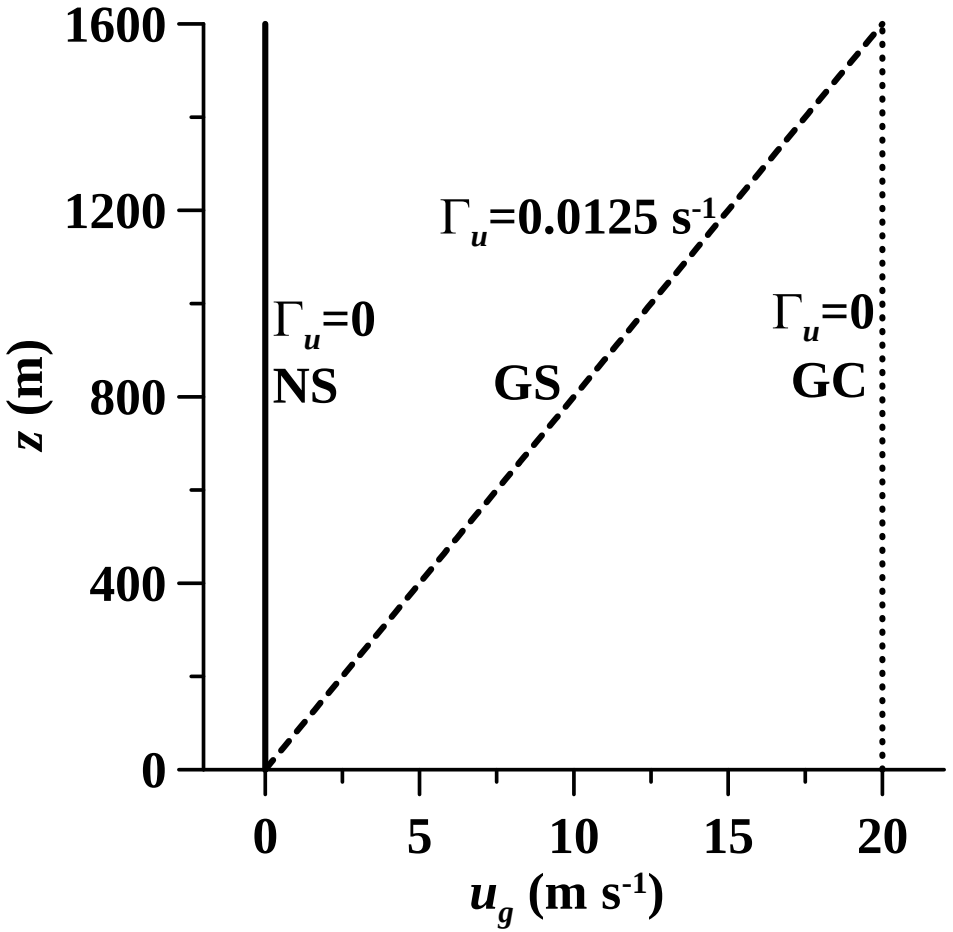

Potential temperature **Wind**

Typical parameters of OU LES for sheared CBL

Parameter	Setting
Domain size	$5.12\times5.12\times1.6\text{km}^3$
Grid	256×256×80
Surface kinematic temperature flux	0.03, 0.1, and 0.3 K m s^{-1}
Temperature stratification above CBL	0.001, 0.003, and 0.010 K m^{-1}
Geostrophic wind	0 m s^{-1} (NS); 20 m s^{-1} (GC) 0 m s^{-1} to 20 m s^{-1} (GS)
Time step	0.5 s (to synchronize NS, GS, and GC cases)
Lateral boundary conditions	Periodic for all prognostic variables and pressure
Top boundary conditions	Neumann for prognostic variables; a sponge layer imposed in the upper 20% of simulation domain
Bottom boundary conditions	No-slip for velocity; Neumann for other prognostic variables; Monin-Obukhov similarity functions implemented locally to relate fluxes and gradients
Subgrid turbulence closure	Subgrid TKE (Deardorff 1980)

Intercomparison of six LES codes for sheared CBL

Organized by Fedorovich and Conzemius in 2004

Participants:

1. School of Meteorology, University of Oklahoma (**OU**): **Evgeni Fedorovich and Robert Conzemius**.
2. National Center for Atmospheric Research (**NCAR**): **Chin-Hoh Moeng and Peter Sullivan**.
3. Department of Mechanical and Aerospace Engineering, West Virginia University (**WVU**): **David Lewellen**.
4. Nansen Environmental and Remote Sensing Center (**NERSC**), Bergen, Norway: **Igor Esau**.
5. Environmental Fluid Mechanics Laboratory, Stanford University, **Fotini Katopodes Chow** used a LES version of the Advanced Regional Prediction System (**ARPS**, Xue et al. 2000, 2001).
6. Institute for Space Studies of Catalonia, Barcelona, Spain, and Department of Meteorology and Air Quality, Wageningen University, Netherlands (**BUW**): **David Pino and Jordi Vilà-Guerau de Arellano**.

Intercomparison of LES for sheared CBLs: $\overline{\theta}$ and $\overline{\theta'\theta'}$

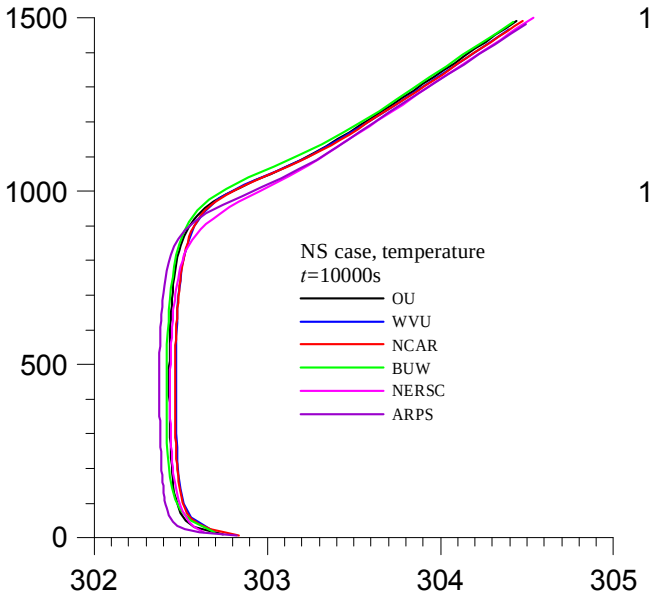

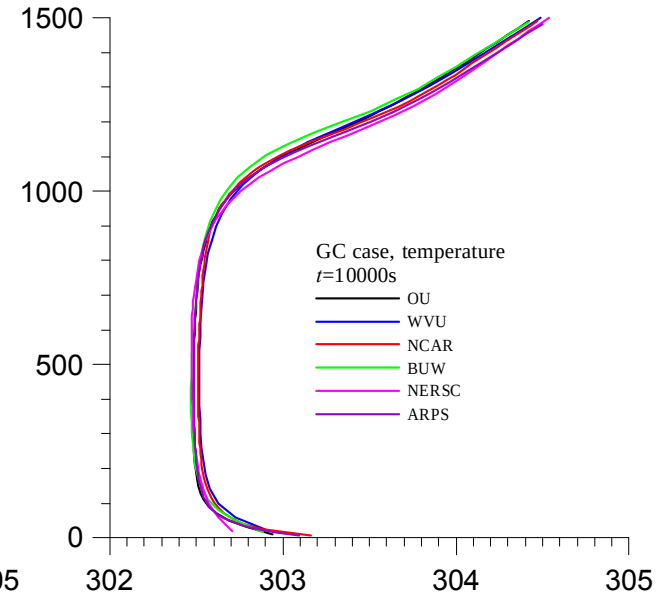

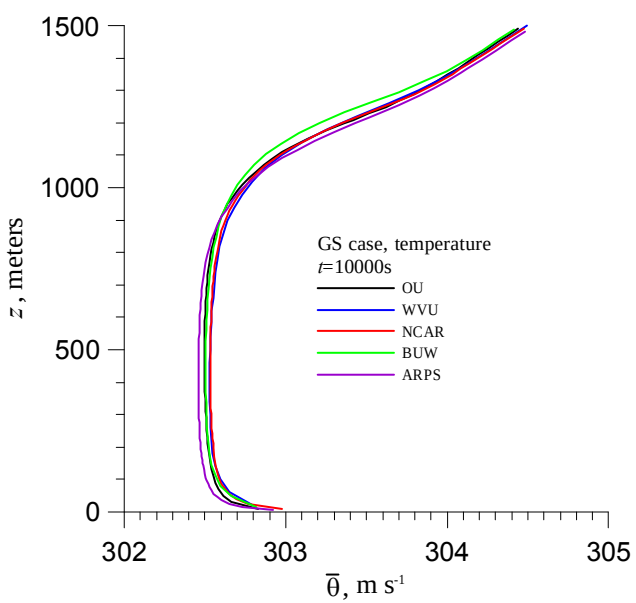

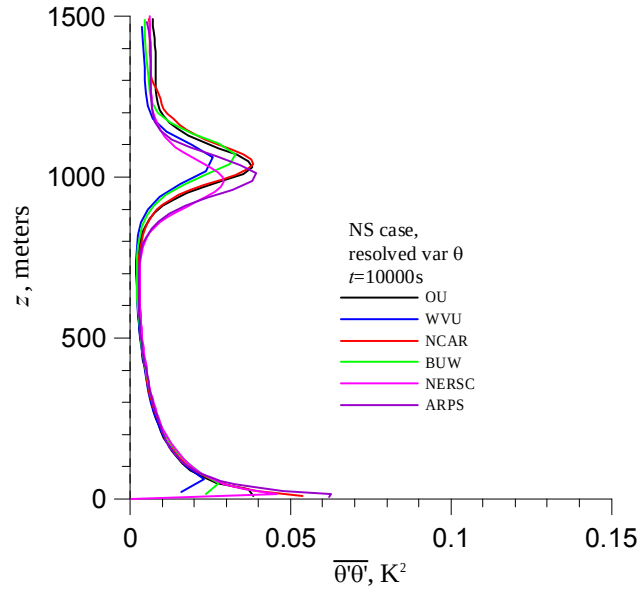

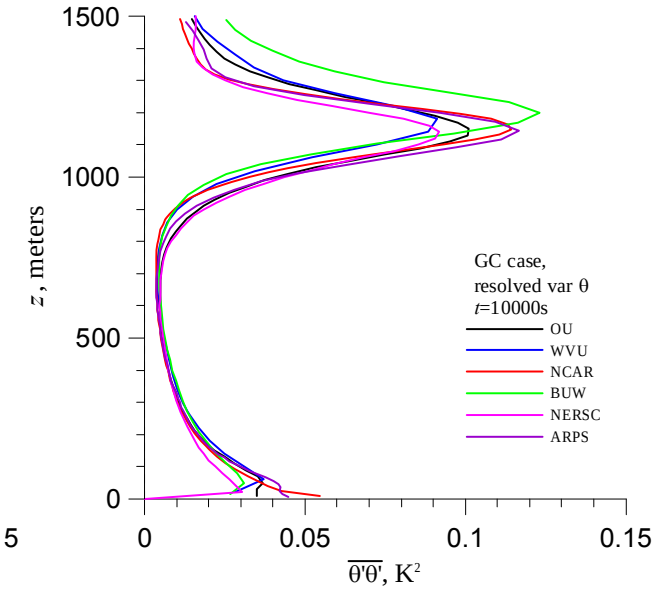

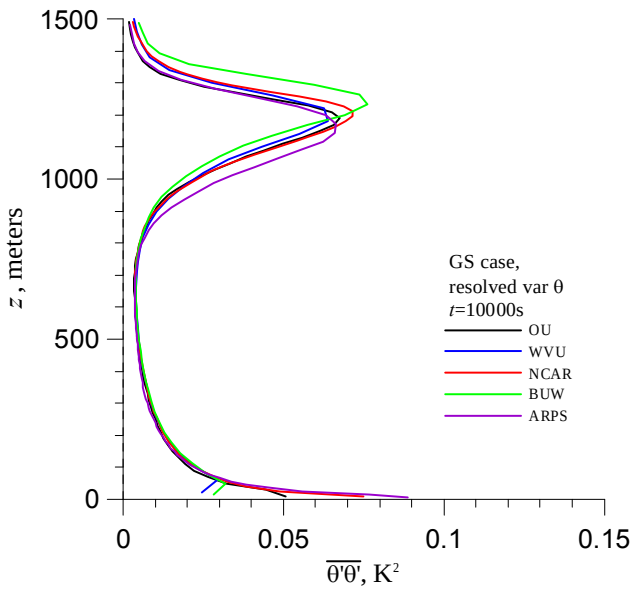

Intercomparison of LES for sheared CBLs: $\overline{u'u'}$ and $\overline{w'w'}$

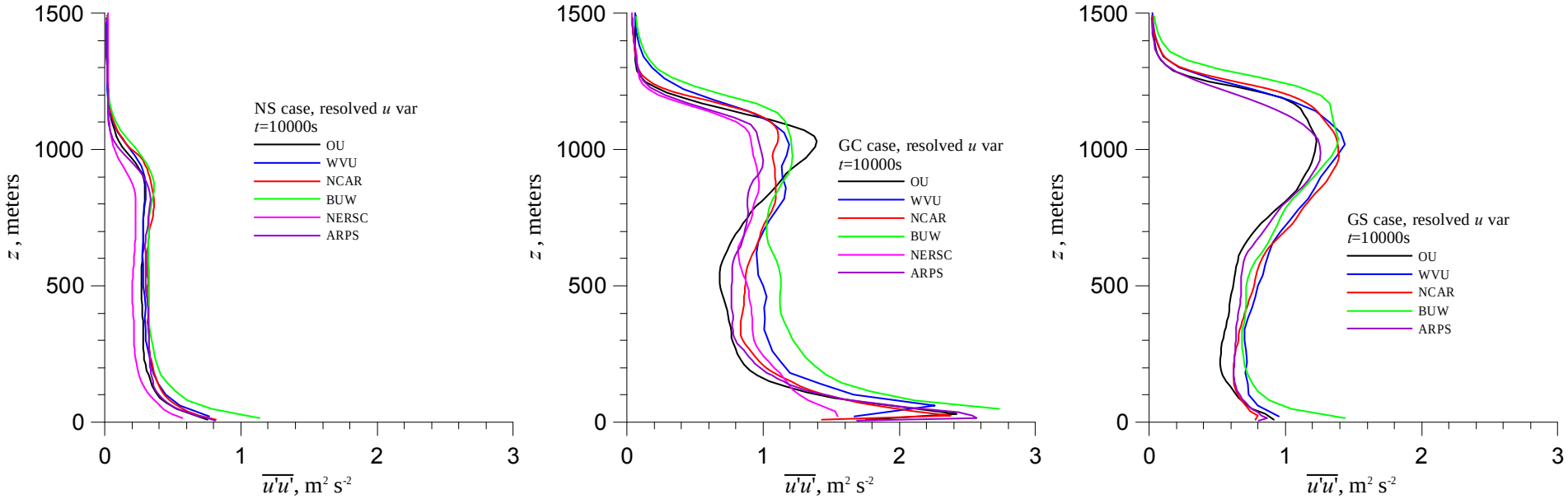

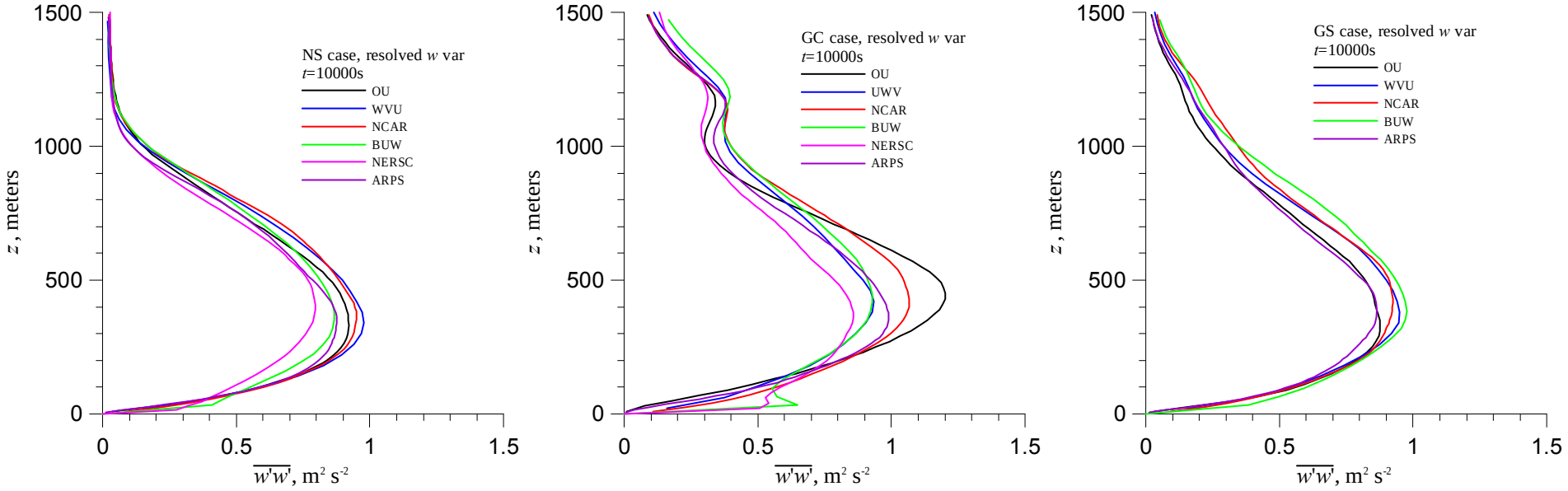

Intercomparison of LES for sheared CBLs: $\overline{w'w'w'}$ and $\overline{\theta'\theta'\theta'}$

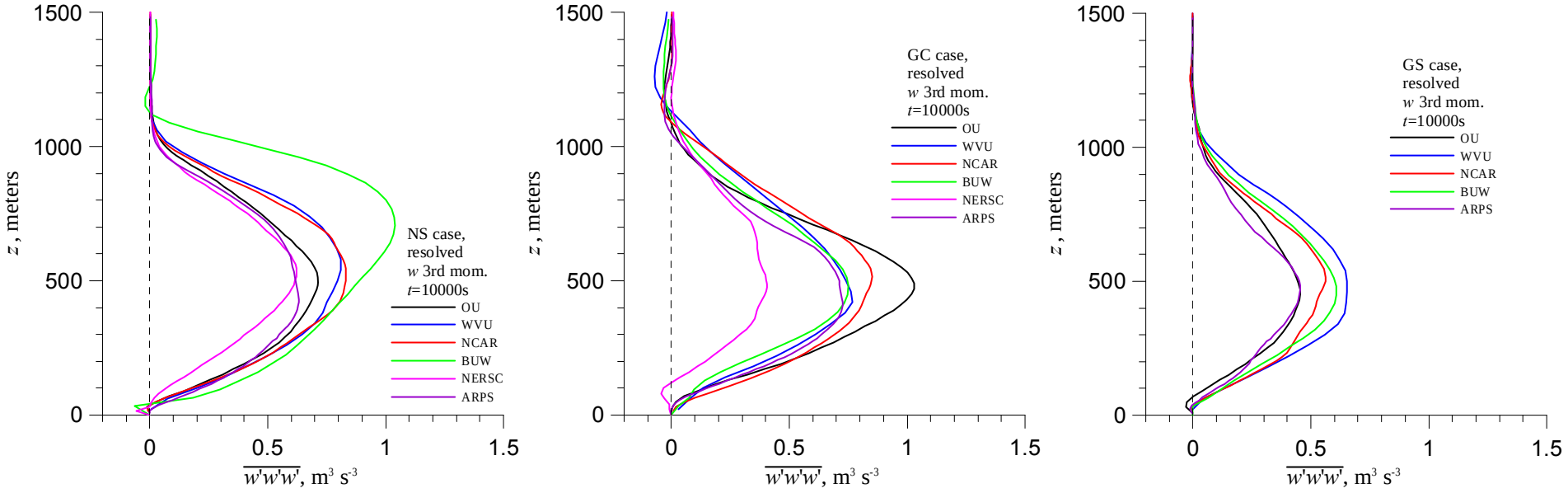

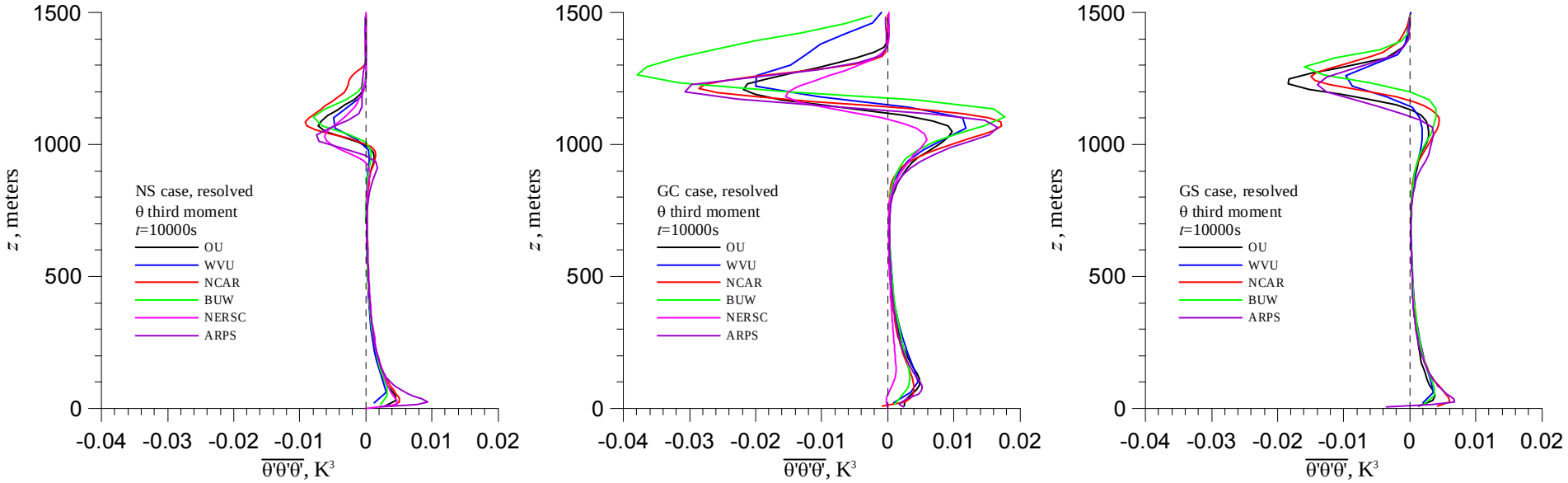

Intercomparison of LES for sheared CBLs: $\overline{u}$, $\overline{v}$, and $\overline{w'u'}$

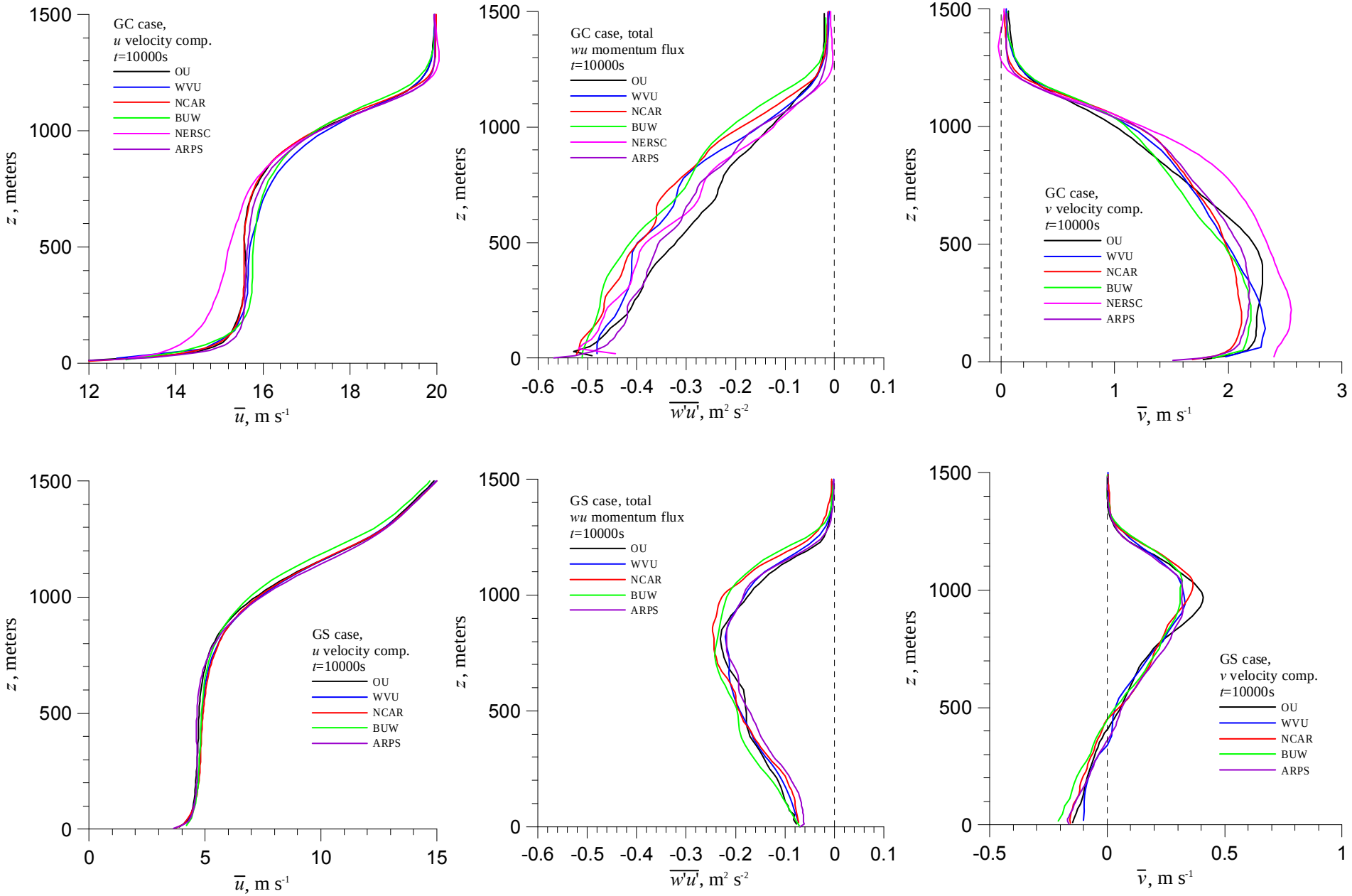

Growth of shear-free CBL: predictions by different LES

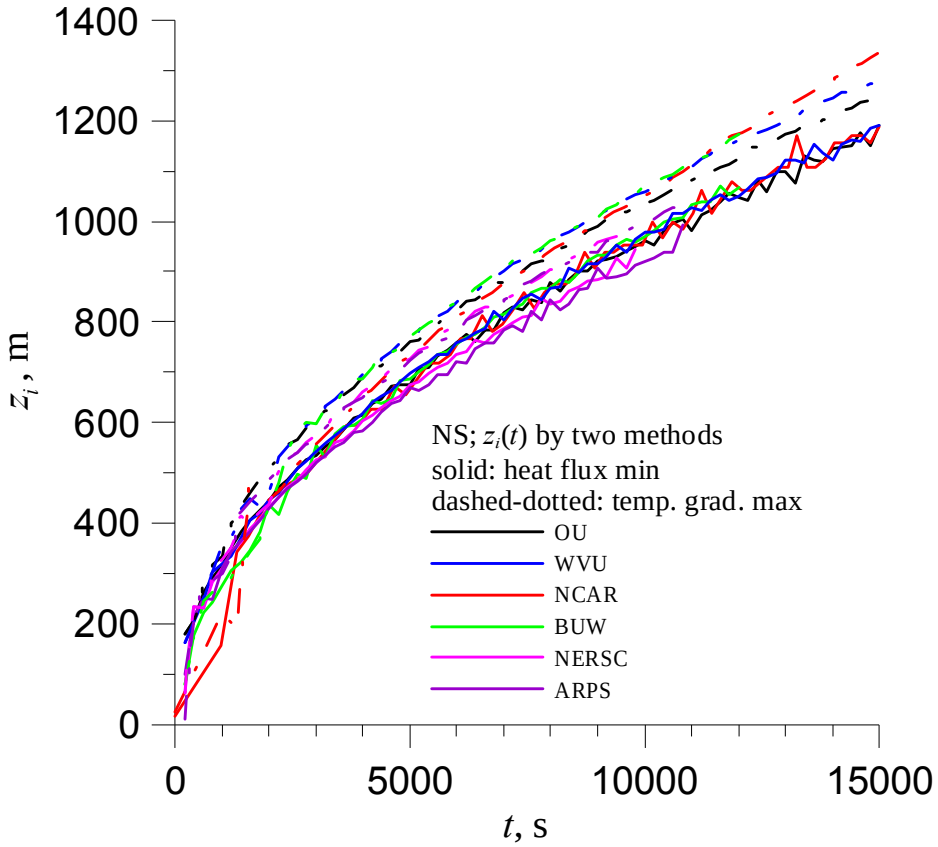

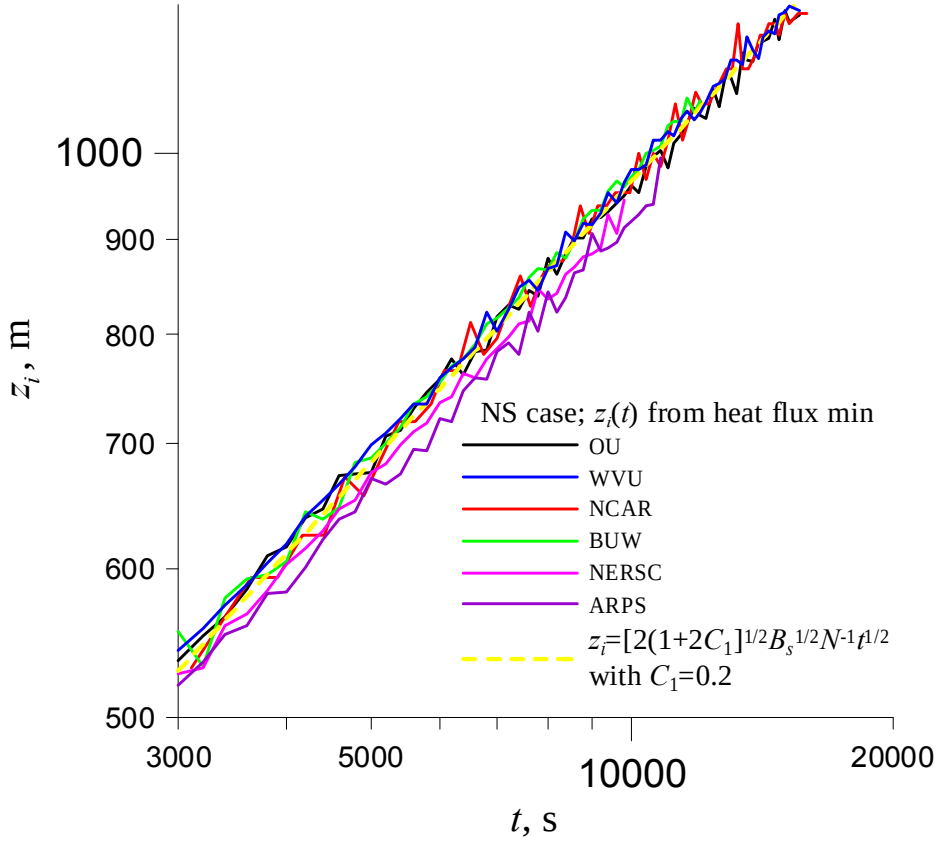

ZOM predicts (see Lecture II): $\hat{z}_i = [2(1+2C_1)\hat{t}]^{1/2},$

where $\hat{z}_i = z_i B_s^{-1/2} N^{3/2}, \hat{t} = tN.$

CBL growth: effects of shear as predicted by different LES

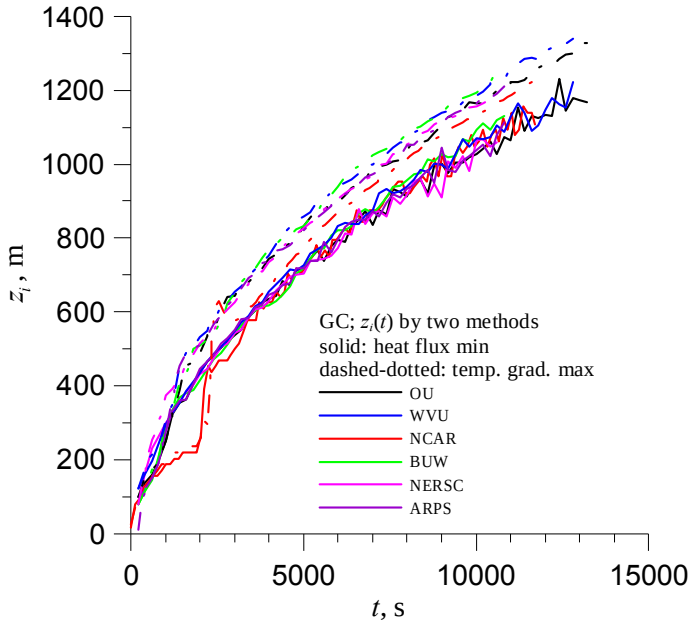

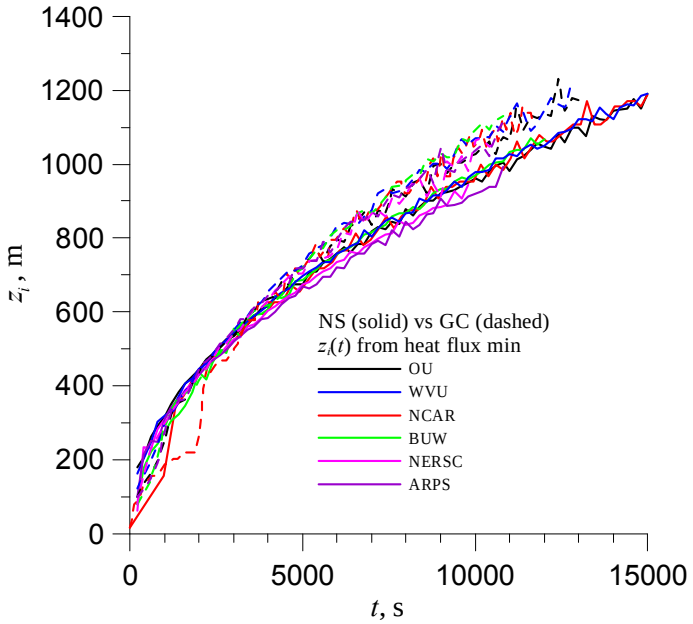

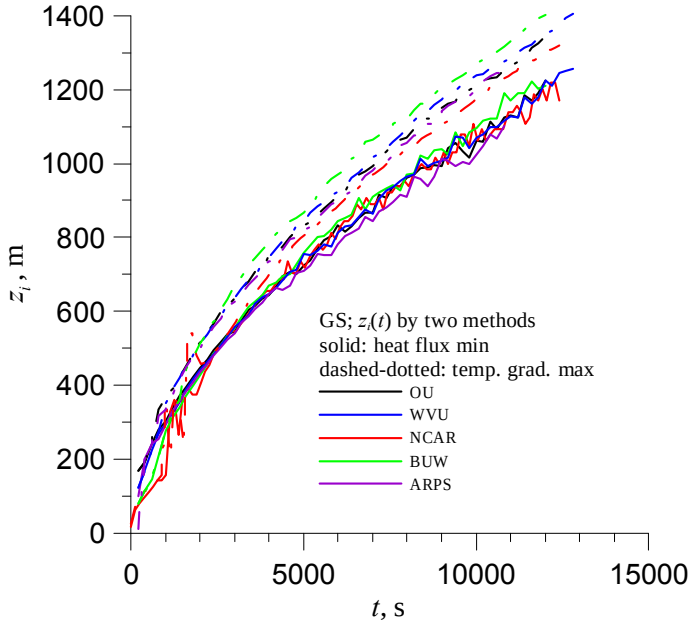

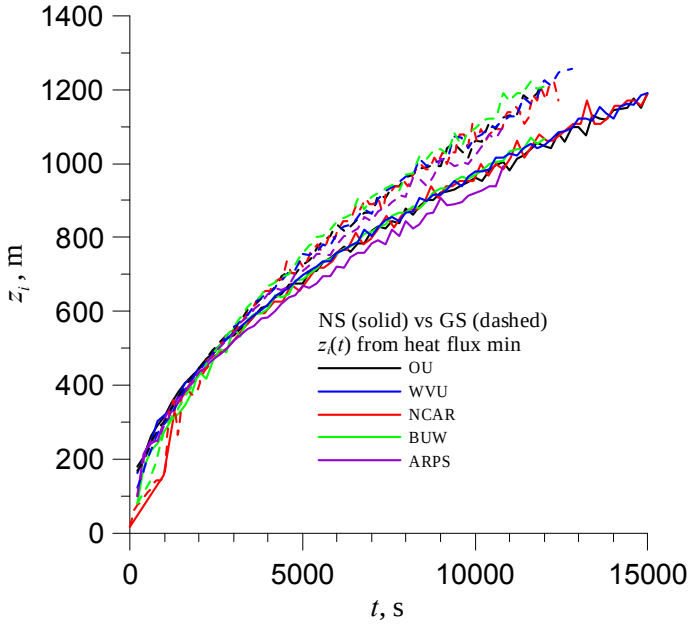

Evolution of CBL depth with different shear and buoyancy forcings

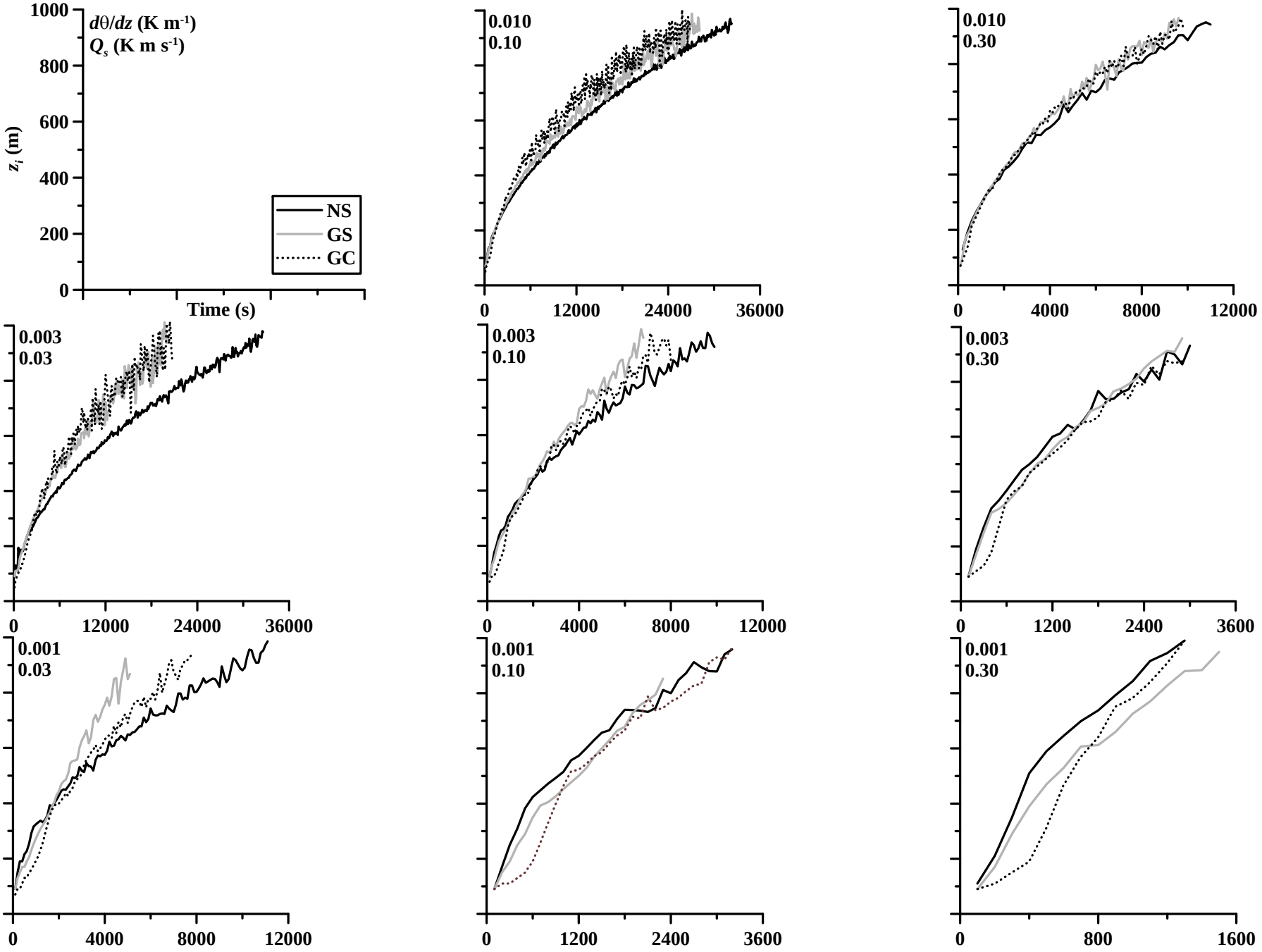

Entrainment flux ratio in CBLs with different shear and buoyancy forcings

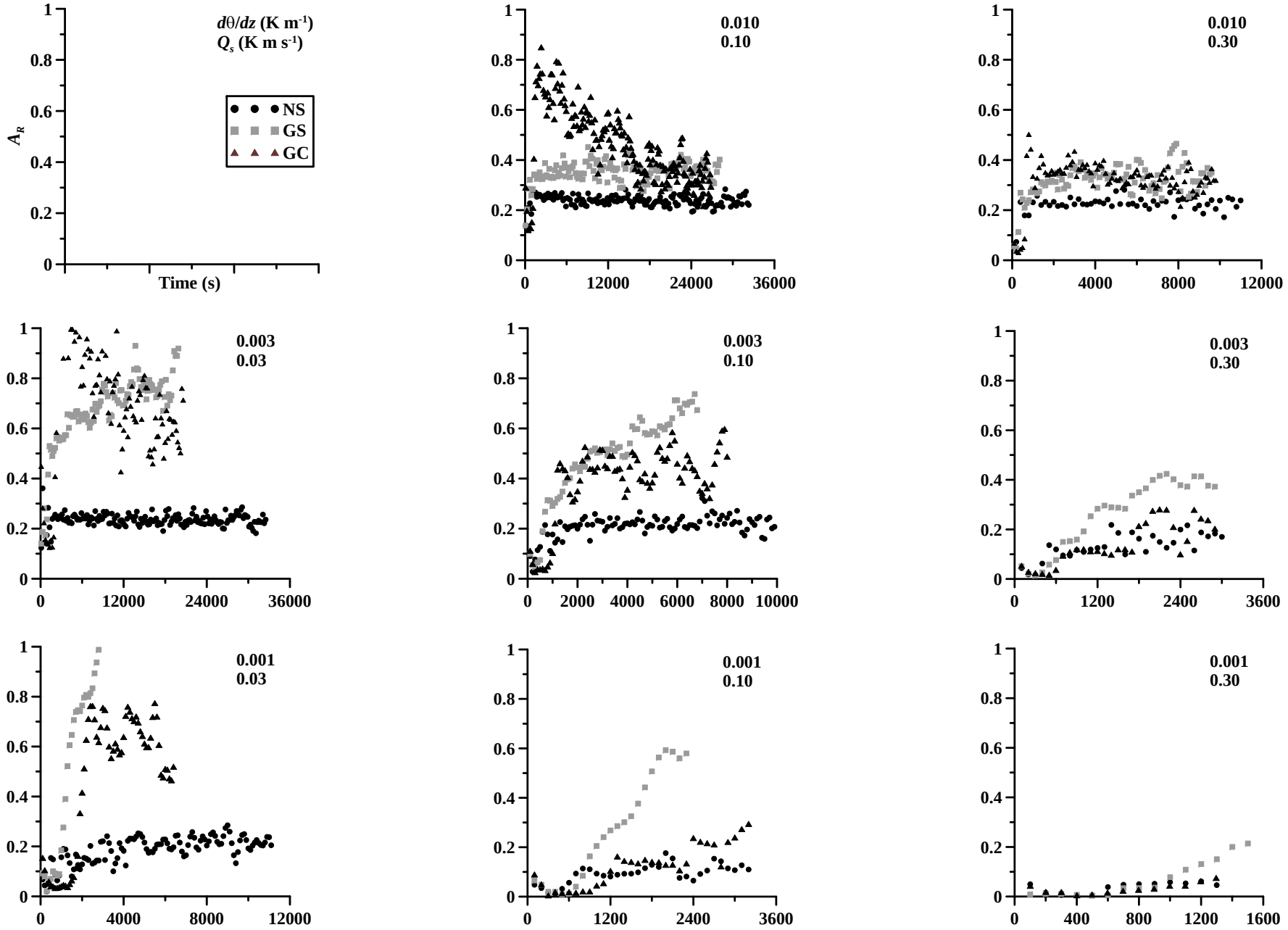

Richardson numbers in entrainment zones of sheared CBLs

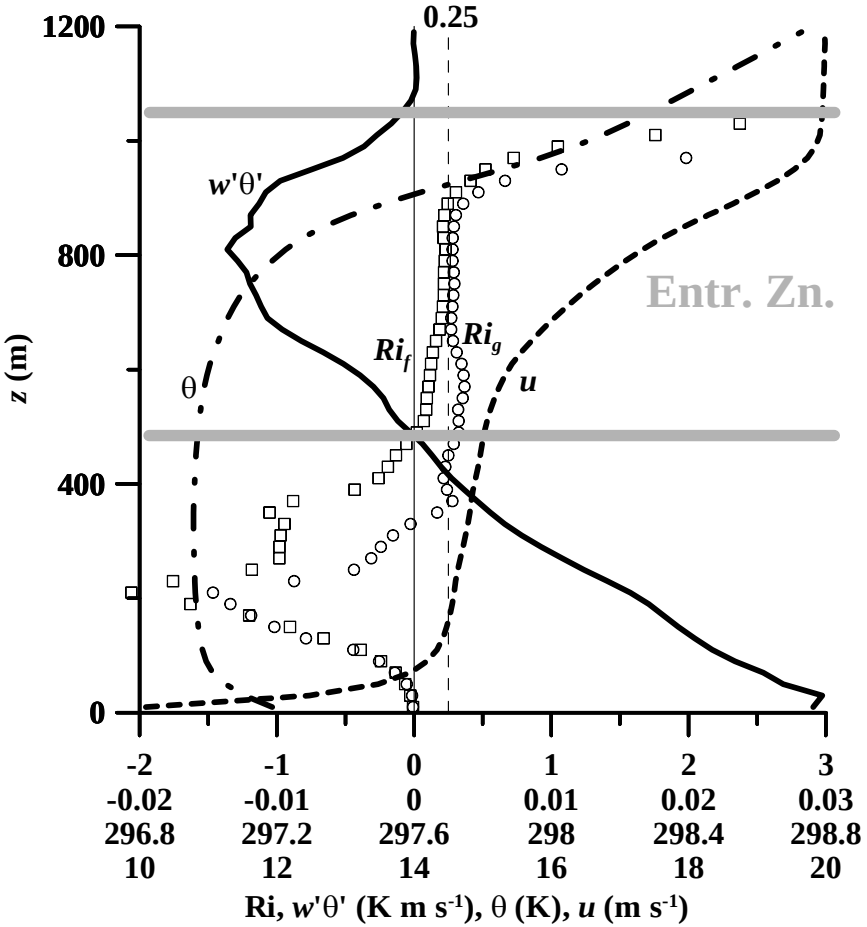

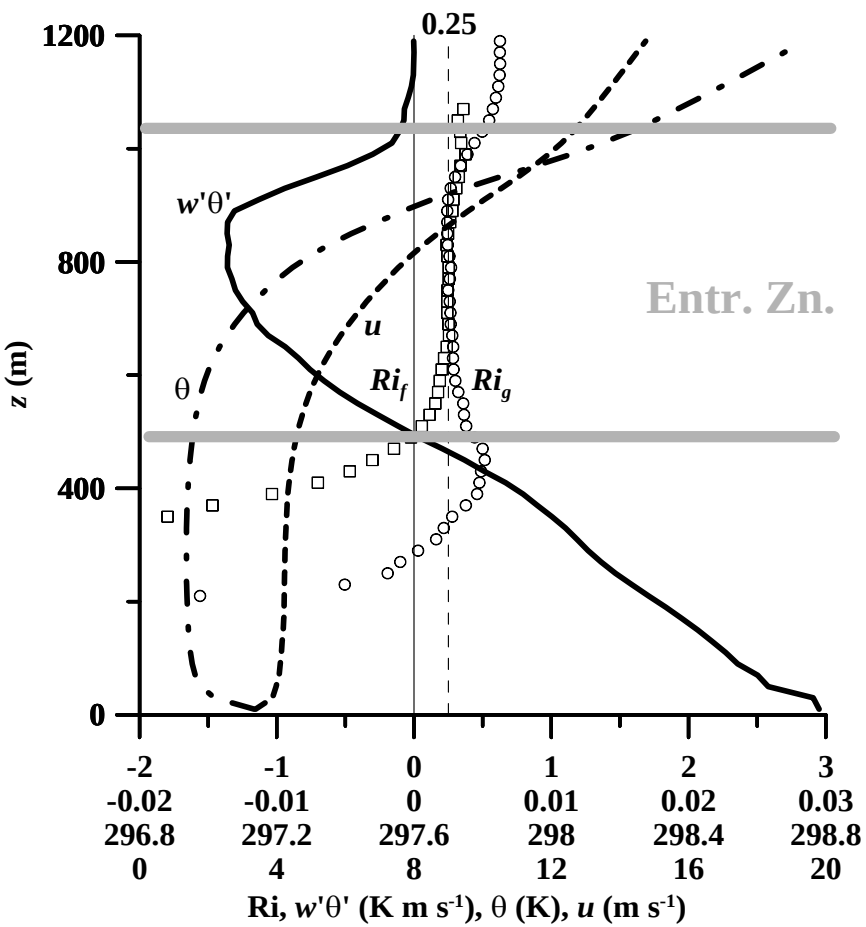

GC (constant geostrophic wind) **GS (height-varying geostrophic wind)**

$$\mathrm{Ri}_g = \frac{\partial b/\partial z}{(\partial u/\partial z)^2 + (\partial v/\partial z)^2}$$ (**gradient Ri**); $$\mathrm{Ri}_f = \frac{B}{\tau_x(\partial u/\partial z) + \tau_y(\partial v/\partial z)}$$ (**flux Ri**)

Constancy of Ri in the upper portion of sheared CBL: observational evidence

(courtesy of Don Lenschow)

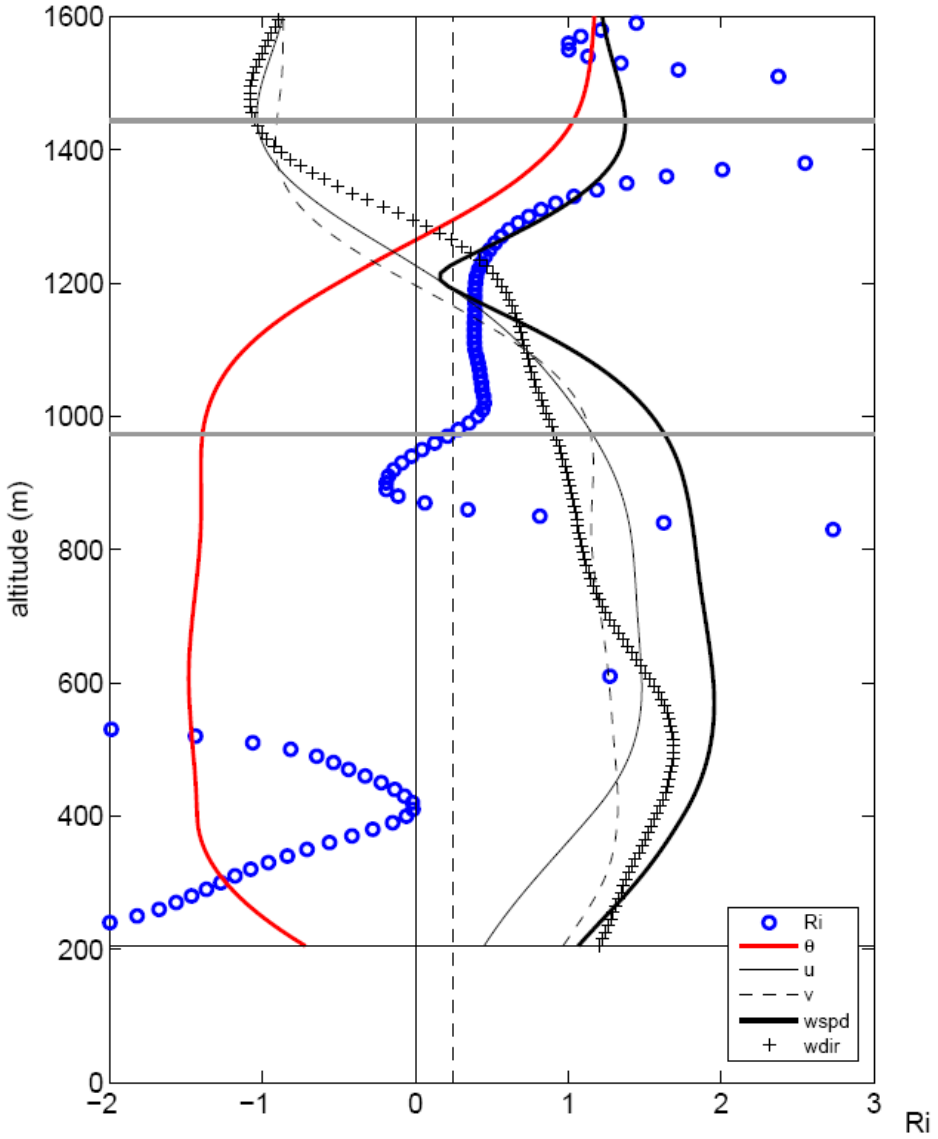

Fraction of shear-generated TKE available for entrainment

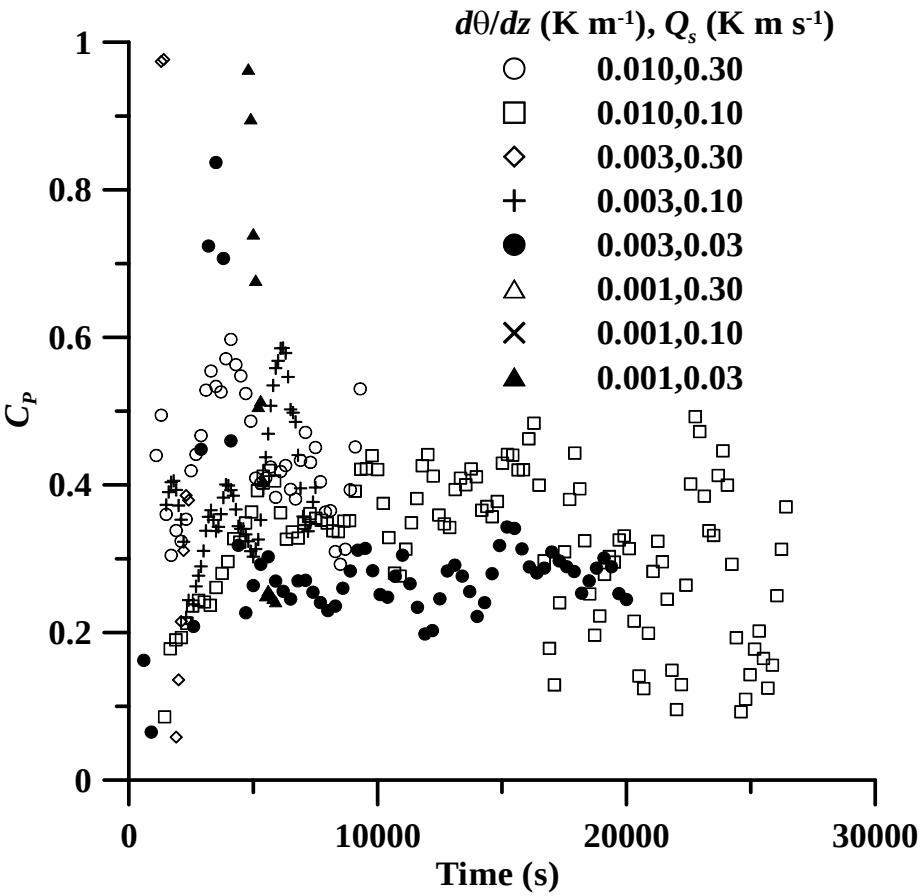

GC (constant geostrophic wind)

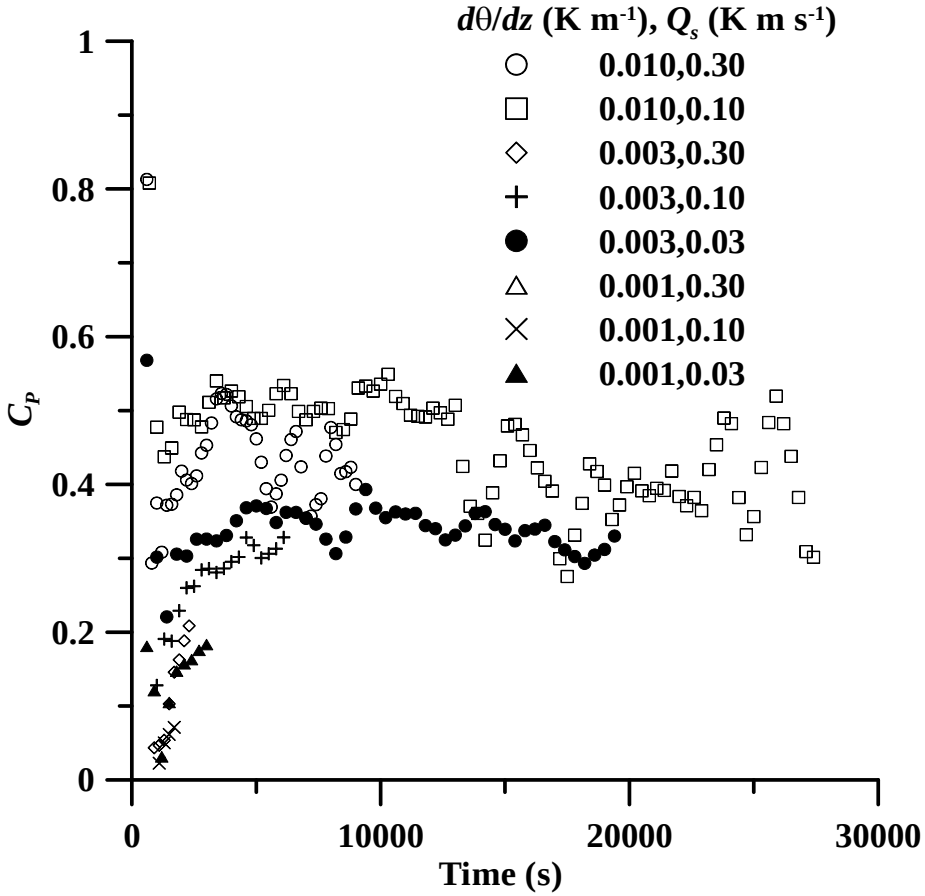

GS (height-varying geostrophic wind)

Fraction of shear-generated TKE available for entrainment:

$$C_P = \frac{\int_0^{z_{iu}} B dz - 0.4 B_s z_i}{\int_{z_{S_{\min}}}^{z_{iu}} \left(\tau_x \frac{\partial u}{\partial z} + \tau_y \frac{\partial v}{\partial z} \right) dz}.$$

Conclusions on turbulence dynamics in sheared CBLs

- Surface layer shear appears to have only an indirect effect on the CBL growth by slowing the flow in the CBL interior and causing the development of shear at the CBL top.
- It is the entrainment zone shear that directly affects the CBL growth.
- Near-top regions of sheared CBLs exhibit sublayers of nearly constant Richardson number within the range from 0.2 to 0.4.
- This feature points to an approximate balance between the TKE generation by shear and the TKE consumption/destruction by negative buoyancy flux.
- Conducted LES indicate that such a balance occurs over a sufficiently deep region within the entrainment layer, so it may be considered characteristic of the whole layer.
- Fraction of the shear-produced TKE used for entrainment is not higher than 0.5; so fractions of 0.7 or higher from previous studies are probably overestimates.

Zero-Order (ZOM) and First-Order (FOM) Models of CBL

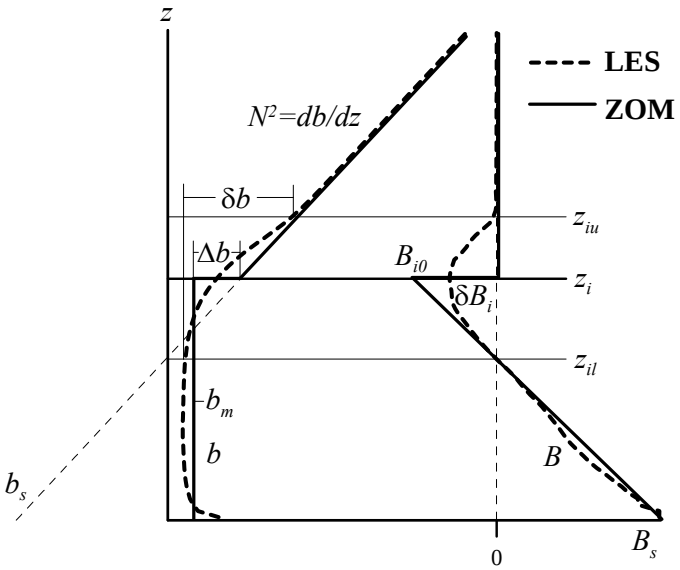

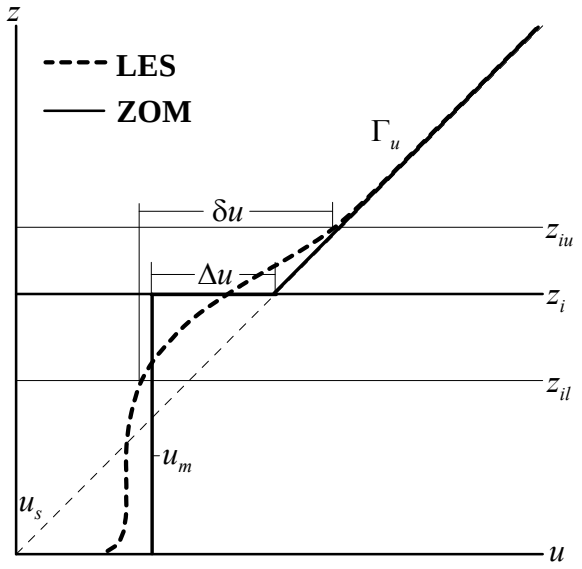

ZOM

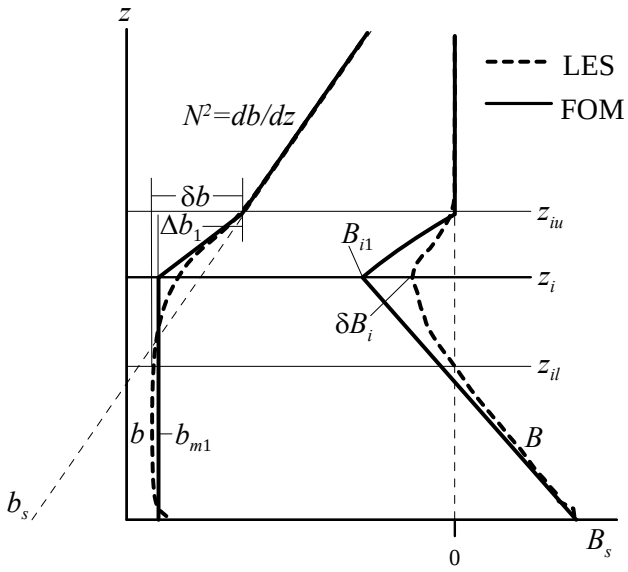

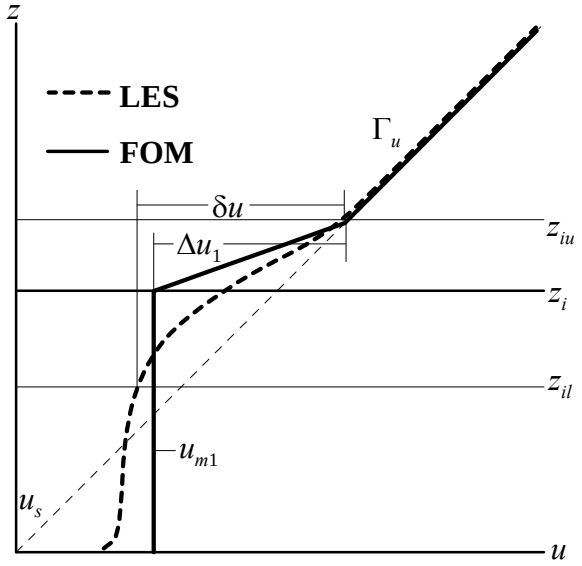

FOM

ZOM-based entrainment parameterization

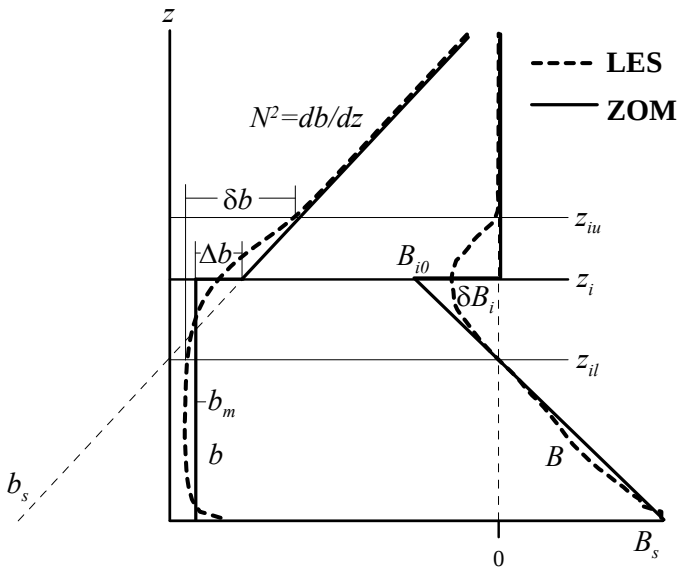

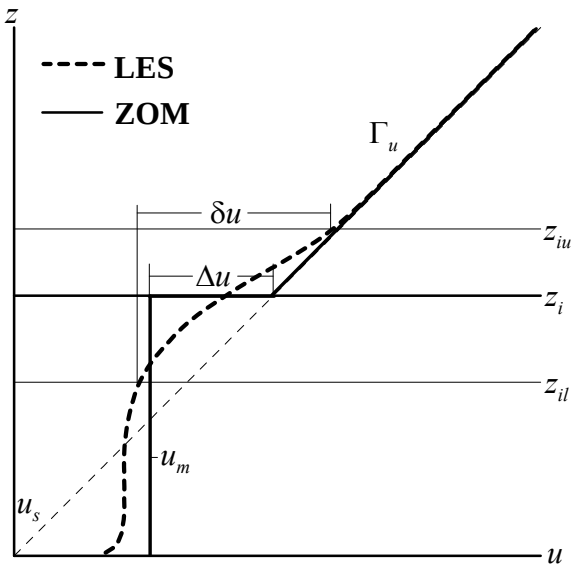

ZOM

ZOM TKE budget (see Lecture II) is given by

$$\frac{d}{dt}\int_0^{z_i} e\,dz = u_m\tau_{xs} + v_m\tau_{ys} + \frac{1}{2}\left(\Delta u^2 + \Delta v^2\right)\frac{dz_i}{dt} + \frac{z_i}{2}\left(B_s - \Delta b\frac{dz_i}{dt}\right) - \Phi_i - \int_0^{z_i}\varepsilon dz.$$

Parameterized CBL growth rate: $$\frac{dz_i}{dt} = \frac{C_1 w_*^3 + C_S u_*^3}{\Delta b z_i + C_T\sigma_w^2 - C_P\left(\Delta u^2 + \Delta v^2\right)}.$$

Tennekes (T73), Zeman and Tennekes (ZT77), Tennekes and Driedonks (TD81), Driedonks (D82), Stull (ST76), Boers et al. (B84), Batchvarova and Gryning (BG94), Pino et al. (PVD03)

Simulation parameters: $\partial\theta/\partial z = 0.003$ K m^{-1}, $Q_s = 0.03$ K m s^{-1}

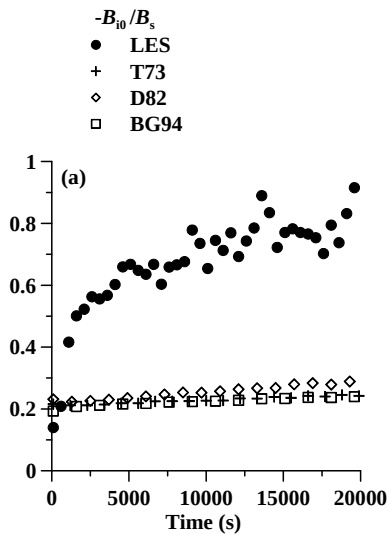

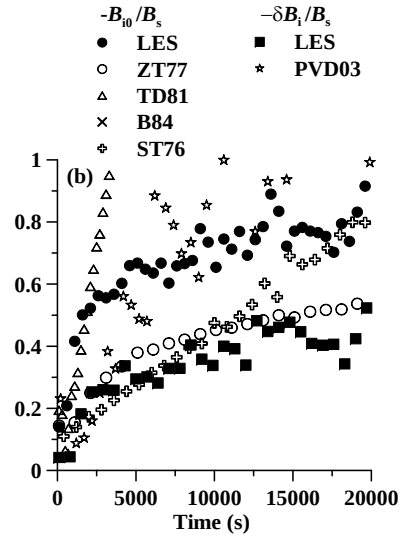

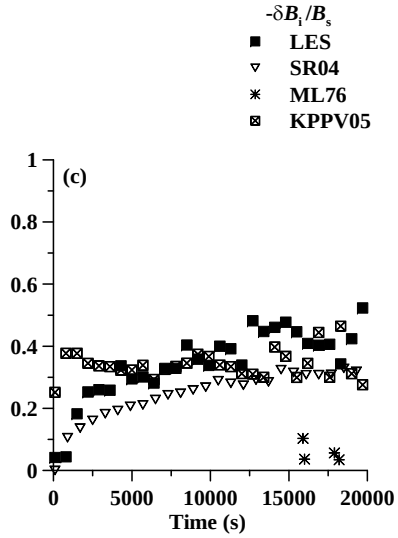

GS

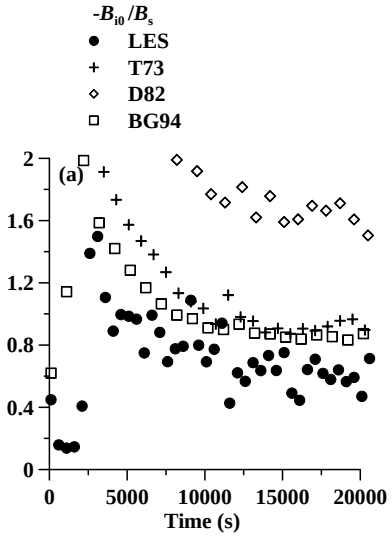

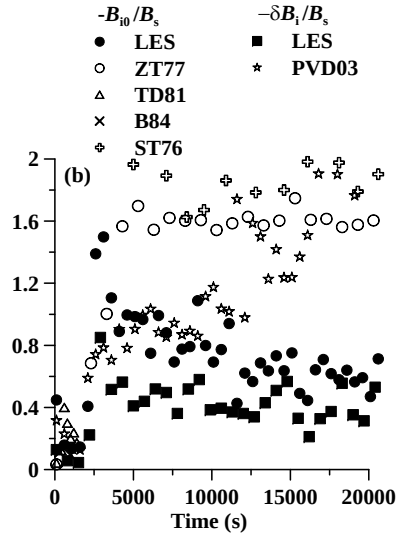

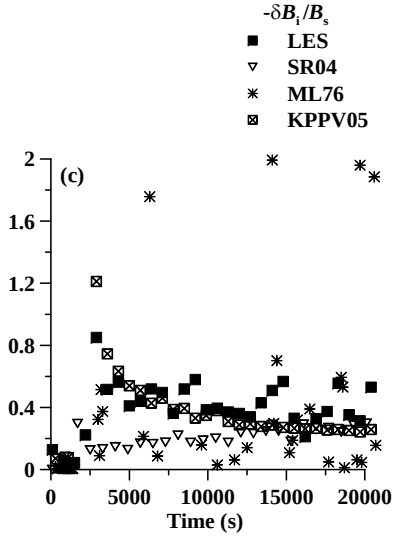

GC

ZOM
surface shear only

ZOM
surface and EZ shear

FOM
and other higher-order models

Conzemius and Fedorovich (2007) hybrid entrainment model

Integrate $\frac{\partial u}{\partial t} = \frac{\partial \tau_x}{\partial z} + f\left(v - v_g\right), \quad \frac{\partial v}{\partial t} = \frac{\partial \tau_y}{\partial z} - f\left(u - u_g\right), \quad \frac{\partial b}{\partial t} = -\frac{\partial B}{\partial z},$

$\frac{\partial e}{\partial t} = \tau_x \frac{\partial u}{\partial z} + \tau_y \frac{\partial v}{\partial z} + B - \frac{\partial \Phi}{\partial z} - \varepsilon,$ **using the FOM representation:**

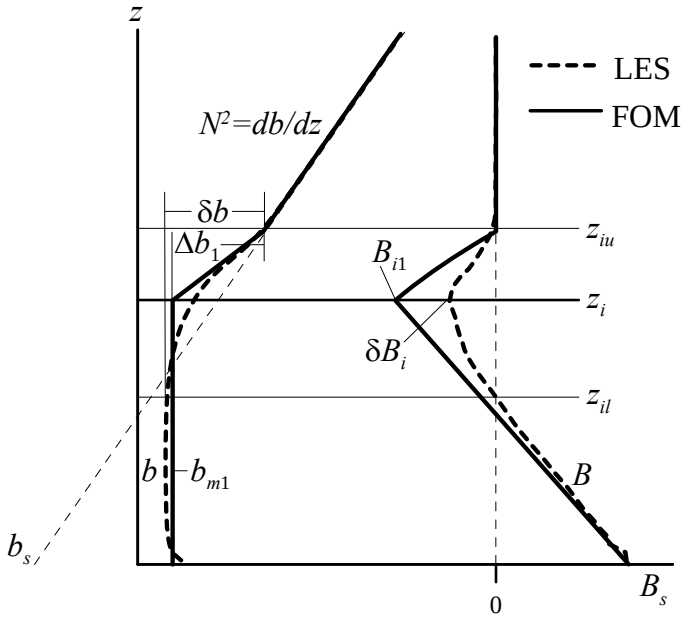

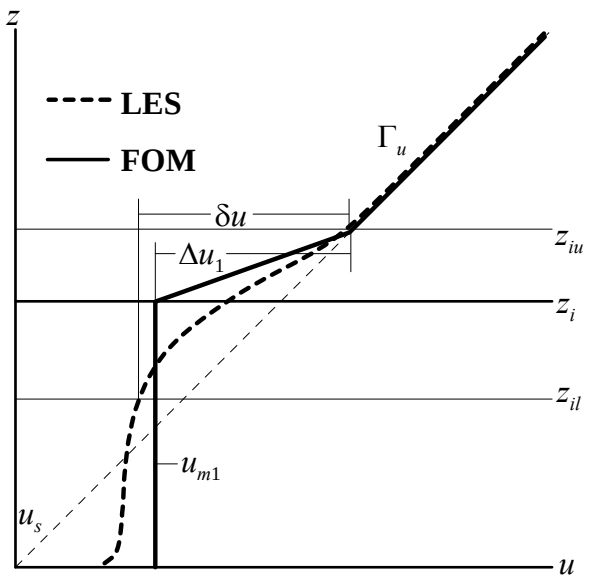

and employ $\mathrm{Ri}_1 = \frac{\Delta z \Delta b_1}{\Delta u_1^2 + \Delta v_1^2} = 0.15$ **to close the problem.**

It is a FOM that reduces to a ZOM when EZ shear is not present!

How well does Conzemius-Fedorovich model work?

Legend →

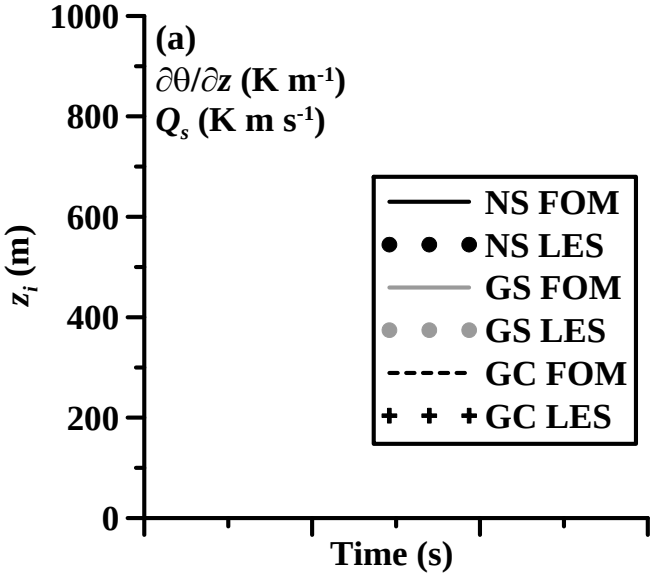

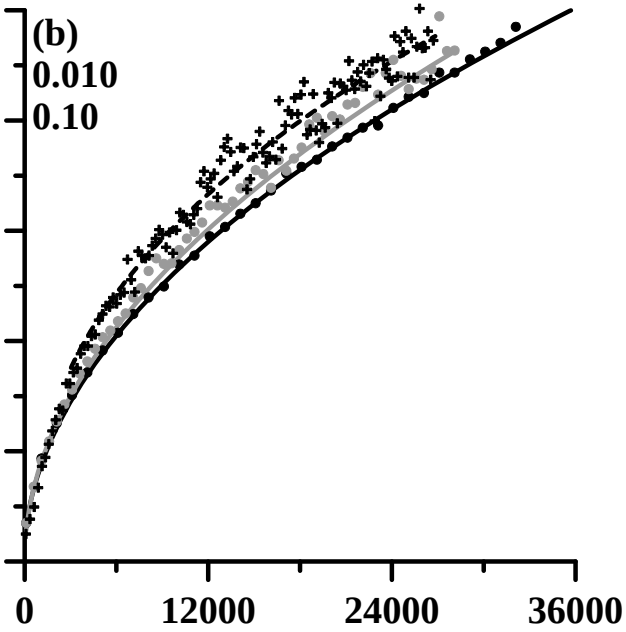

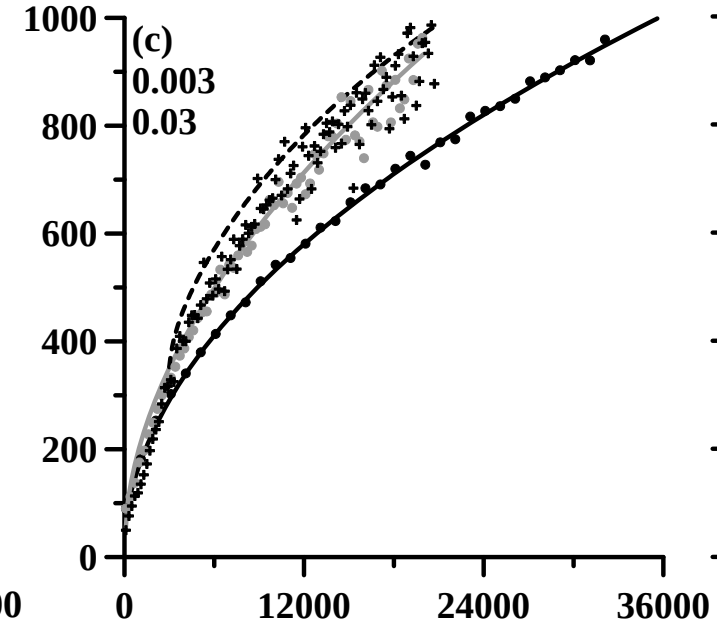

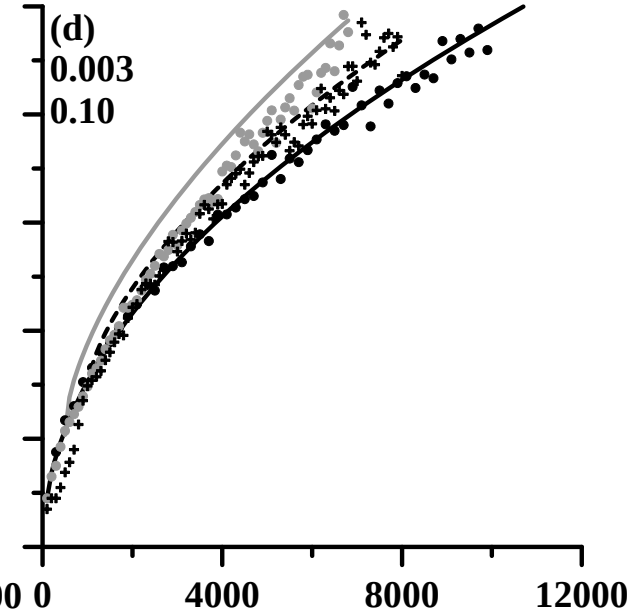

Conclusions on performance of bulk CBL models

- Most of ZOM- and FOM-based parameterizations suggested to-date overestimate entrainment in CBLs with strong shear.
- In the ZOM and FOM entrainment formulas, effect of the entrainment-zone shear is often represented by a negative-sign term in the denominator which makes solutions unstable.
- Fraction of shear-produced TKE that is available for entrainment appears to be smaller than is usually assumed in the models.
- The fraction of surface-generated TKE available for entrainment can be set to zero in bulk entrainment parameterizations.
- Parameterizations that include only the surface layer shear often perform well in CBL cases with height-constant geostrophic forcing; the surface friction in these cases acts as a proxy for the entrainment zone shear effect.
- Including Richardson-number constraint in the representation of the entrainment zone shear appears to improve the ability of bulk parameterizations to reproduce the sheared CBL entrainment.

References

Conzemius, R. J., and E. Fedorovich, 2006a: Dynamics of sheared convective boundary layer entrainment. Part I: Methodological background and large-eddy simulations. *J. Atmos. Sci*., **63**, 1151-1178.

Conzemius, R. J., and E. Fedorovich, 2006b: Dynamics of sheared convective boundary layer entrainment. Part II: Evaluation of bulk model predictions of entrainment flux. *J. Atmos. Sci*., **63**, 1179-1199.

Conzemius, R., and E. Fedorovich, 2007: Bulk models of the sheared convective boundary layer: evaluation through large eddy simulations. *J. Atmos. Sci.*, **64**, 786-807.

Fedorovich, E., and R. Conzemius, 2008: Effects of wind shear on the atmospheric convective boundary layer structure and evolution. *Acta Geophysica*, **56**, 114-141.

Fedorovich, E., R. Conzemius, I. Esau, F. Katopodes Chow, D. Lewellen, C.-H. Moeng, D. Pino, P. Sullivan, and J. Vilà-Guerau de Arellano, 2004: Entrainment into sheared convective boundary layers as predicted by different large eddy simulation codes. Preprints, *16th Symp. on Boundary Layers and Turbulence*, Amer. Meteor. Soc., 9-13 August, Portland, Maine, USA, CD-ROM, P4.7.

Available at: http://weather.ou.edu/~fedorovi/fedorovich.html

Thanks to

Bob Conzemius (my former Ph.D. student, OU)

Flow structure in sheared vs. shear-free CBL

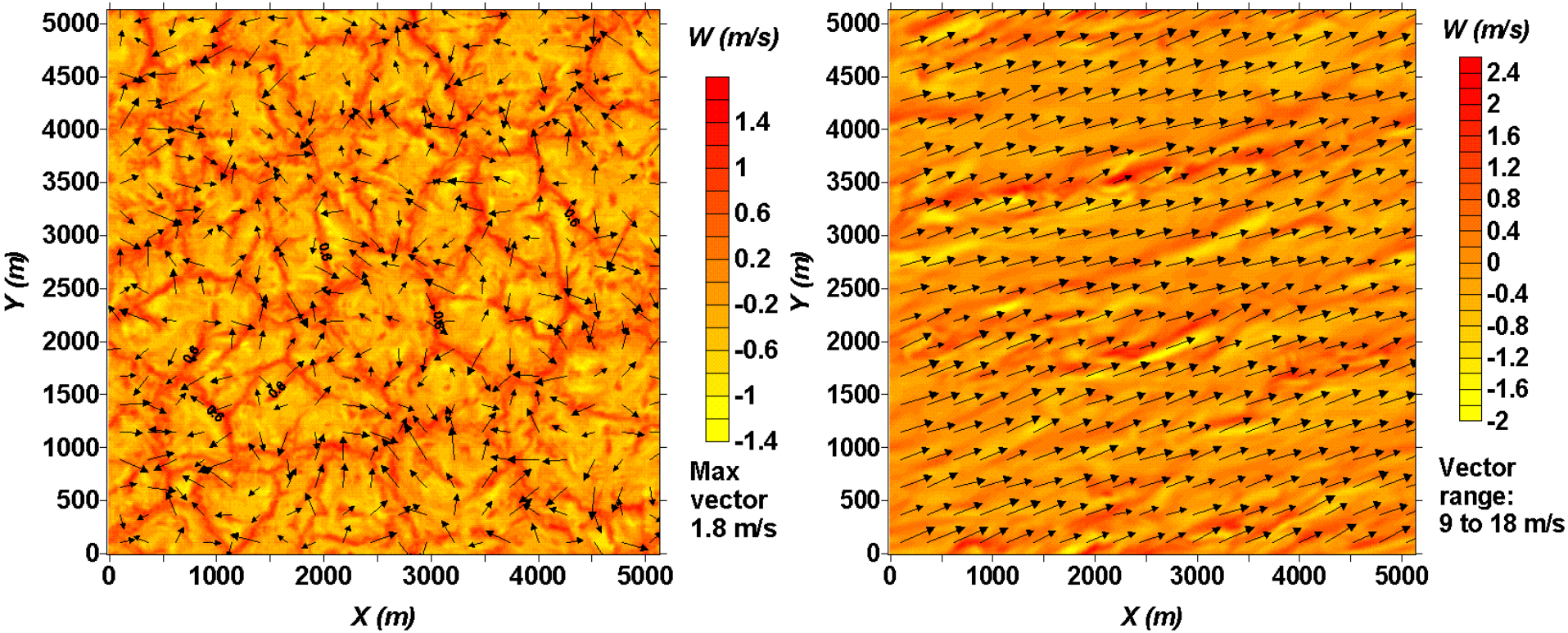

Shear-free CBL **Sheared CBL**

Vectors: u and v; color scale: w